

UNITED STATES NAVAL POSTGRADUATE SCHOOL



THESIS

SIMULATION OF FULL AND PART-LOAD PERFORMANCE
OF A FREE-PISTON GAS GENERATOR
BY ELECTRONIC ANALOG METHODS

Alan F. Barnes

DUDLEY KNOX LIBRARY
NAVAL POSTGRADUATE SCHOOL
MONTEREY CA 93943-5101

SIMULATION OF FULL AND PART-LOAD PERFORMANCE
OF A FREE-PISTON GAS GENERATOR
BY ELECTRONIC ANALOG METHODS

.

* * * * *

Alan F. Barnes

SIMULATION OF FULL AND PART-LOAD PERFORMANCE
OF A FREE-PISTON GAS GENERATOR
BY ELECTRONIC ANALOG METHODS

by

Alan F. Barnes

//

Lieutenant Commander, United States Navy

Submitted in partial fulfillment of
the requirements for the degree of

MASTER OF SCIENCE
IN
MECHANICAL ENGINEERING

United States Naval Postgraduate School
Monterey, California

1960

NPS Archive
1960
Barnes, A.

~~Thesis~~
B229

SIMULATION OF FULL AND PART-LOAD PERFORMANCE
OF A FREE-PISTON GAS GENERATOR
BY ELECTRONIC ANALOG METHODS

by

Alan F. Barnes

This work is accepted as fulfilling
the thesis requirements for the degree of

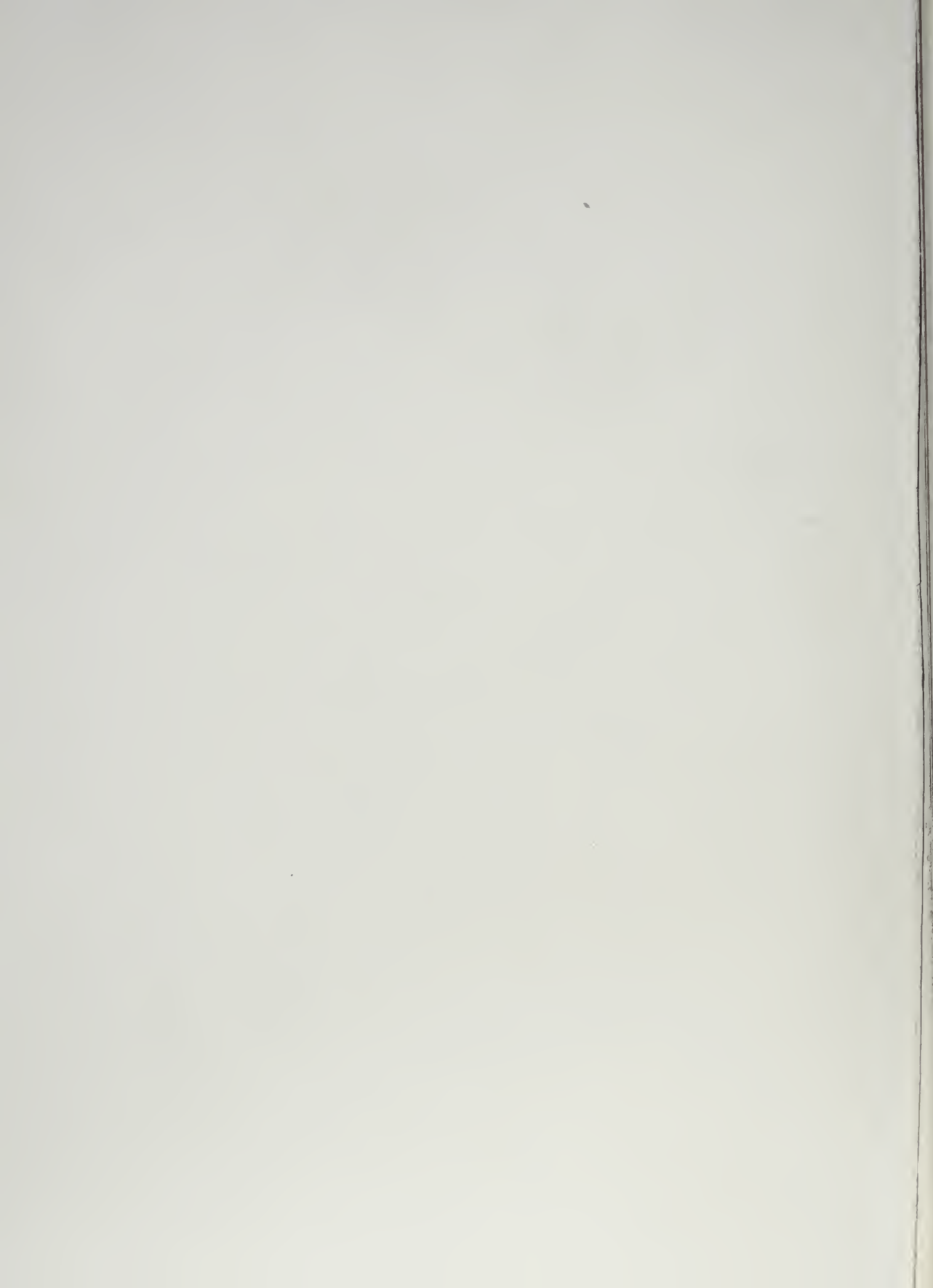
MASTER OF SCIENCE

IN

MECHANICAL ENGINEERING

from the

United States Naval Postgraduate School



ABSTRACT

In this investigation, use was made of an electronic analog for simulating the operation of a free-piston gas generator. The basic concept of the analog was developed in a previous investigation and involved the creating of the various free-piston forces as functions of displacement and integrating these combined forces in accordance with Newton's second law of motion to obtain a solution representing piston motion - all by electronic analog means.

Modifications were made to the basic analog circuit of the previous investigation to overcome an unstable operating condition. The modified circuit was then employed for determining performance characteristics of an actual free-piston gas generator under varied load conditions.

The results of these studies showed that the operation of a free-piston gas generator could be simulated to a reasonable degree of accuracy and stability by use of an electronic analog and that this method might be a valuable means for design and performance predictions of free-piston engine systems.

ACKNOWLEDGMENT

The writer wishes to express his appreciation for the assistance and encouragement given him by Professor Paul F. Pucci of the U. S. Naval Postgraduate School during this investigation. He is also indebted to the Department of Mathematics and Mechanics of the U. S. Naval Postgraduate School for use of the Boeing Electronic Analog Computer.

TABLE OF CONTENTS

Section	Title	Page
1.	Introduction	1
2.	Characteristics of the Free-Piston Engine System	3
3.	Dynamics of Piston Motion	6
4.	General Electronic Analog of the Free-Piston Gas Generator	9
5.	System Inputs, Parameters and Performance Relations	12
6.	Electronic Analog of the Two-Stroke Standard Diesel Cycle	19
7.	Electronic Analog of the Reciprocating Compressor	25
8.	Electronic Analog of the Bounce Cylinder "Gas Spring"	27
9.	Electronic Analog of the Friction Force	29
10.	Electronic Analog of the Free-Piston Gas Generator	30
11.	Operating Characteristics of the Free-Piston Gas Generator	32
12.	Simulation of Full and Part Load Performance of the SIGMA GS-34 Free-Piston Gas Generator on the Analog Computer	35
13.	Conclusions	56
14.	Bibliography	58
Appendix I	Time and Magnitude Scaling	60
Appendix II	Programming Analog Computer for SIGMA GS-34 Free-Piston Gas Generator - Full and Part Load	62
Appendix III	Full and Part Load Performance Calculations from Computer Solution Results	66
Appendix IV	Analog Computer Symbols	74
Appendix V	Description of Equipment	76

LIST OF ILLUSTRATIONS

Figure		Page
1.	Basis Applications of the Free-Piston System	4
2.	Spring-Mass Analog for Free-Piston Gas-Generator System	6
3.	Forces Acting on the Free Piston	7
4.	Basic Electronic Analog Computer Arrangement for Free-Piston Gas Generator	11
5.	Illustration of Displacement and Clearance Parameters for Pistons in Contact at Midpoint	13
6.	Electronic Analog of the Two-Stroke Standard Diesel Cycle	22
7.	Electronic Analog of the Reciprocating Compressor	26
8.	Electronic Analog of the Bounce Cylinder "Gas Spring"	28
9.	Electronic Analog of the Friction Force	29
10.	Electronic Analog of the Free-Piston Gas Generator	31
11.	Pressure versus Displacement Diagram for Engine Cylinder at Full Load	39
12.	Pressure versus Displacement Diagram for Compressor Cylinder at Full Load	40
13.	Pressure versus Displacement Diagram for Bounce Cylinder at Full Load	40
14.	Pressure versus Displacement Diagram for Engine Cylinder at Three-Quarters Load	43
15.	Pressure versus Displacement Diagram for Compressor Cylinder at Three-Quarters Load	44
16.	Pressure versus Displacement Diagram for Bounce Cylinder at Three-Quarters Load	44
17.	Pressure versus Displacement Diagram for Engine Cylinder at One-Half Load	45
18.	Pressure versus Displacement Diagram for Compressor Cylinder at One-Half Load	46

1
2
3
4
5
6
7
8
9
10
11
12
13
14
15
16
17
18
19
20
21
22
23
24
25
26
27
28
29
30
31
32
33
34
35
36
37
38
39
40
41
42
43
44
45
46
47
48
49
50
51
52
53
54
55
56
57
58
59
60
61
62
63
64
65
66
67
68
69
70
71
72
73
74
75
76
77
78
79
80
81
82
83
84
85
86
87
88
89
90
91
92
93
94
95
96
97
98
99
100

Figure		Page
19.	Pressure versus Displacement Diagram for Bounce Cylinder at One-Half Load	46
20.	Pressure versus Displacement Diagram for Engine Cylinder at One-Quarter Load	47
21.	Pressure versus Displacement Diagram for Compressor Cylinder at One-Quarter Load	48
22.	Pressure versus Displacement Diagram for Bounce Cylinder at One-Quarter Load	48
23.	Thermal Efficiency on LHV Basis of Combined Gasifier-Turbine System versus Load from Computer Solution Results	49
24.	Fuel Consumption versus Load from Computer Solution Results	50
25.	Turbine Inlet Pressure and Temperature versus Load from Computer Solution Results	51
26.	Frequency and Gas Flow Rate versus Load from Computer Solution Results	52
27.	Operating Pressures versus Load Employed in Computer Simulation of SIGMA GS-34 Gas Generator	53
28.	Inner and Outer Dead Points as Measured from Midpoint of Engine Cylinder versus Load from Computer Solution Results	54
29.	Ratio of Air/Fuel and Engine/Compressor Air versus Load from Computer Solution Results	55
30.	Actuation of Relays	77
31.	Equipment Components Employed in Investigation	79

The first part of the document discusses the importance of maintaining accurate records of all transactions. It emphasizes that every entry should be supported by a valid receipt or invoice. This ensures transparency and allows for easy verification of the data. The text also mentions that regular audits are necessary to identify any discrepancies or errors in the accounting system.

In addition, the document highlights the need for a clear and concise reporting structure. Management should be provided with timely and accurate financial statements that clearly show the company's performance over a specific period. This information is crucial for making informed decisions and for communicating the company's financial health to stakeholders.

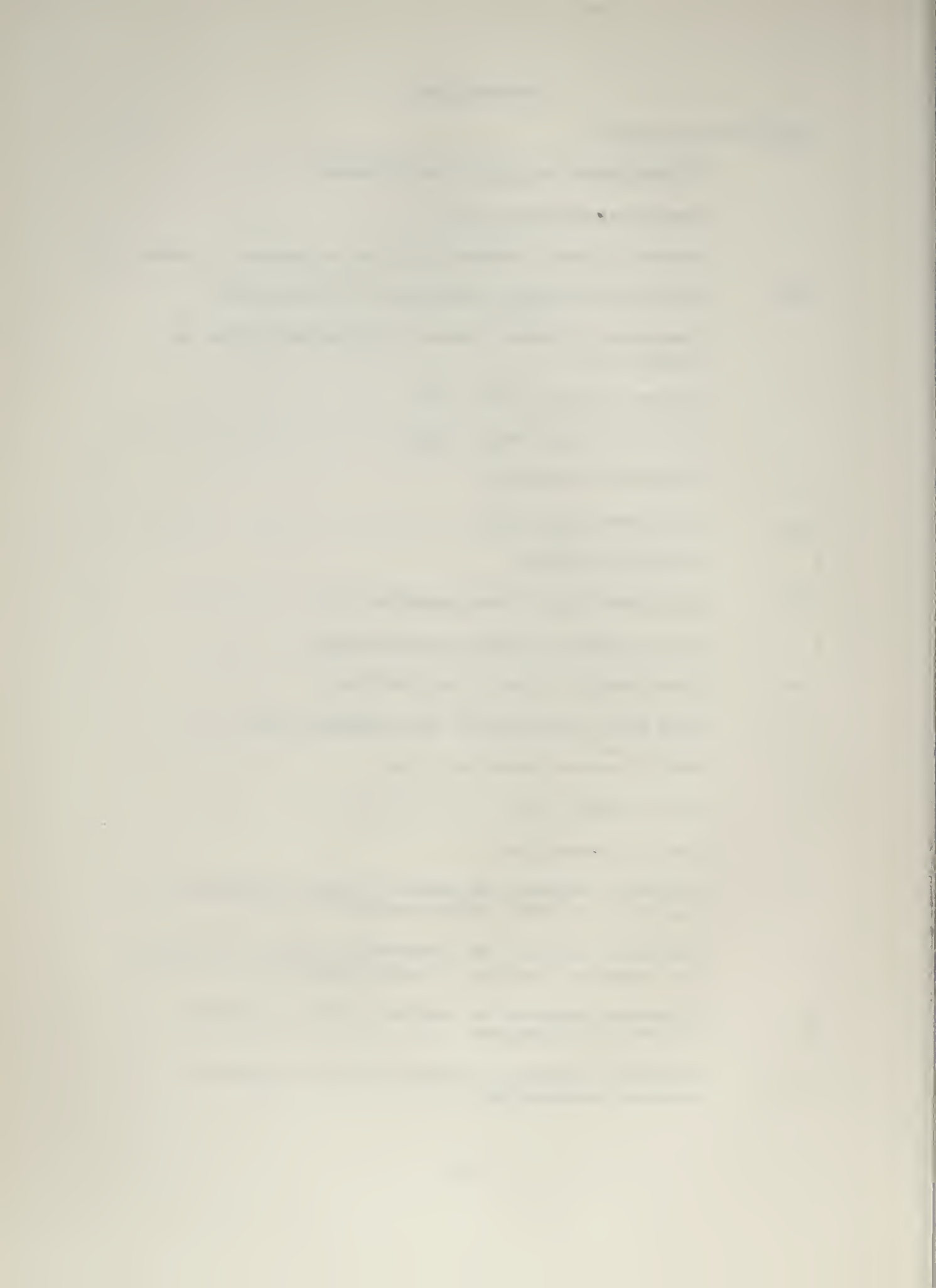
Furthermore, the document stresses the importance of maintaining up-to-date financial records. This includes not only the current year's data but also historical records for comparison and trend analysis. Proper record-keeping is essential for compliance with tax regulations and for providing a clear audit trail.

Finally, the document concludes by stating that a strong financial foundation is key to the long-term success of any business. By adhering to these principles of accurate record-keeping and transparent reporting, companies can build trust, manage risk, and achieve their financial goals.

NOMENCLATURE

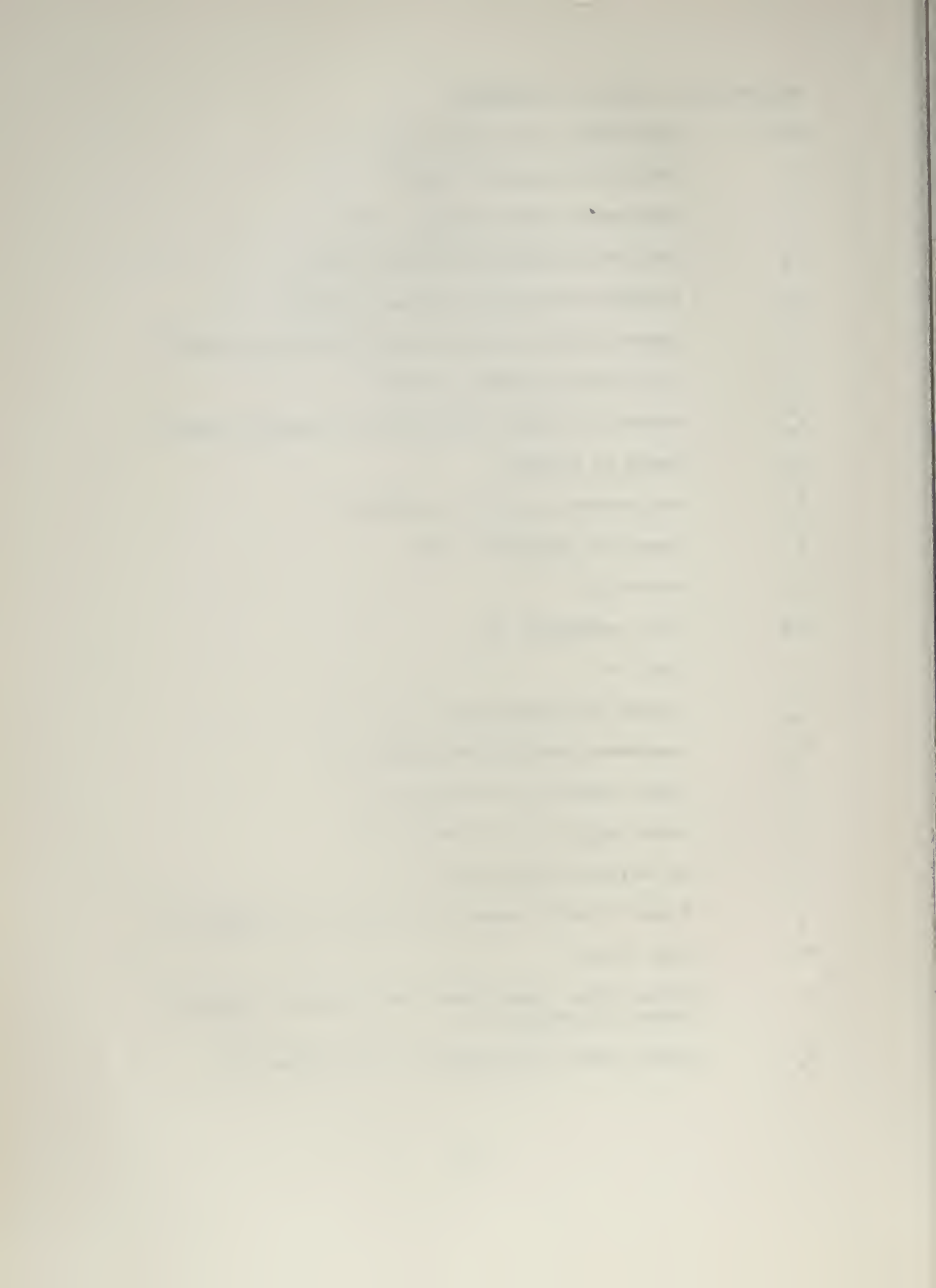
English Letter Symbols:

- a - Potentiometer constant, dimensionless
- A - Cross-sectional area, ft^2
- b - Bounce cylinder clearance with engine pistons in contact, ft
- BSFC - Brake specific fuel consumption, lbm fuel/shphr
- c - Compressor cylinder clearance with engine pistons in contact, ft
- C - Coulomb friction force, lbf
- C - Electrical capacitance, μfd
- f_r - Frequency, cycles/min
- F_{fr} - Frictional force, lbf
- h - Enthalpy, BTU/lbm
- IDP - Inner dead point piston position, ft
- k - Ratio of specific heats, dimensionless
- LHV - Lower heating value of fuel, BTU/lbm
- m_d - Mass of air delivered by the compressor, lbm
- m_e - Mass of engine intake air, lbm
- m_f - Mass of fuel, lbm
- M - Mass of piston, lbm
- n_b - Polytropic exponent for bounce cylinder compression and expansion processes, dimensionless
- n_c - Polytropic exponent for compression cylinder compression and expansion processes, dimensionless
- n_e - Polytropic exponent for engine cylinder compression process, dimensionless
- n'_e - Polytropic exponent for engine cylinder expansion process, dimensionless



English Letter Symbols (continued)

ODP	- Outer dead point piston position, ft
P_o	- Ambient air pressure, lbf/ft ²
P_i	- Compressor intake pressure, lbf/ft ²
P_d	- Compressor discharge pressure, lbf/ft ²
P_s	- Scavenge air receiver pressure, lbf/ft ²
P_p	- Engine cylinder pressure during scavenging, lbf/ft ²
P_t	- Gas delivery pressure, lbf/ft ²
P_b^o	- Maximum or initial bounce cylinder pressure, lbf/ft ²
Q_f	- Energy of fuel, BTU
R	- Gas constant for air, ft-lbf/lbm-°R
R	- Electrical resistance, ohms
s	- Stroke, ft
shp	- Shaft horsepower, hp
t	- Time, sec
T_o	- Ambient air temperature, °R
T_d	- Compressor discharge temperature, °R
T_e	- Engine exhaust gas temperature, °R
T_p	- Engine intake air temperature, °R
T_t	- Gas delivery temperature, °R
V_p	- Engine cylinder volume at point of port closure, ft ³
Wk	- Work, ft-lbf
x	- Engine piston displacement from midpoint or point of contact of pistons, ft
x_p	- Engine piston displacement at port closure, ft



English Letter Symbols (continued)

- $\dot{x}, \dot{y}, \dot{z}$ - Piston velocity, ft/sec
- \ddot{x} - Piston acceleration, ft/sec²
- y - Compressor piston displacement from compressor cylinder head, ft
- Y_i - Length of air intake portion of compressor stroke, ft
- z - Bounce piston displacement from bounce cylinder head, ft

Subscripts:

- b - Refers to bounce cylinder
- c - Refers to compressor cylinder
- e - Refers to engine cylinder
- f - Refers to operational amplifier feedback
- s - Refers to isentropic process

Greek Letter Symbols:

- α_i - Magnitude scaling factor, units of i/volt
- α_t - Time scaling factor, computer time/real time
- Δ - Difference, dimensionless
- ϵ - Relay bias voltage, volts
- η - Efficiency, percent

Miscellaneous:

- \bar{i} - Scaled computer voltage quantity - related to real physical quantity, i, by scale factor, α_i - thus $i = \alpha_i \bar{i}$

1. Introduction

An electronic analog of the operation of a free-piston gas generator or gasifier based on the "spring-mass" nature of the free-piston engine system was undertaken by LT Arthur E. PLOW, USN. [1]¹ In that investigation, the first law of thermodynamics was solved on an analog computer three concurrent times representing electronic analogs of an internal combustion engine, a reciprocating compressor, and a bounce cylinder "gas spring". Friction forces were also introduced. The results of these four analogs were combined and integrated in accordance with Newton's second law of motion to yield a solution representing piston motion. In addition a comparison of analog computer solution results and actual performance data at approximate rated output conditions was also made for the SIGMA² organization of France model GS-34 free-piston gasifier.

The results of LT PLOW's investigation showed that the various nonlinear "gas-spring" forces of the gasifier (engine, compressor and bounce cylinder forces) as well as a friction force could be simulated by electronic analog methods. The operation of the bounce cylinder analog, however, was non-stable or drifting and tended to disrupt the problem. The inaccuracy of this analog resulted from errors in a two-quadrant electronic multiplication performed in this circuit, these errors being due to the inherent inability of an electronic multiplier to give uniform results in multiplications involving more than one quadrant (i.e. both inputs having the same sign).

¹Numerals in brackets refer to bibliography.

²Société Industrielle Générale de Mécanique Appliquée (SIGMA),
Venissieux, France.

Relatively few techniques for predicting the design and performance of free-piston engine systems may be found in the available literature. These, for the most part, involve rather complex numerical processes as illustrated by London's [2] thermodynamic-dynamic analysis of a free-piston gas generator system in which a calculated "basic design" may be extrapolated by certain affinity relations to different plant capacities and dimensions.

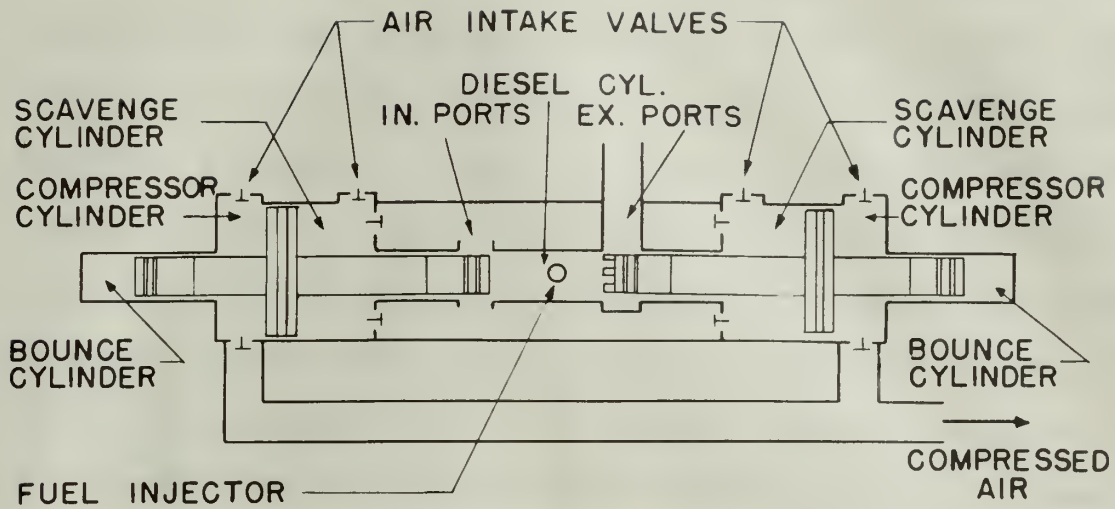
In this investigation the electronic analog method as developed by PLOW [1] but modified for stability of operation was employed for determining performance characteristics of a free piston gas generator under varied load conditions. To this end full and partial load studies were made of the SIGMA GS-34 gasifier by introducing appropriate fixed geometric and variable operating parameters to the analog problem. This procedure could be adapted as well to performance predictions of modified gas generator designs and thus would be of considerable benefit in the development of different sized machines.

In the available literature there is little information on prediction of part load behavior of a free-piston gas generator. The analog method might well be a useful means in this type of analysis.

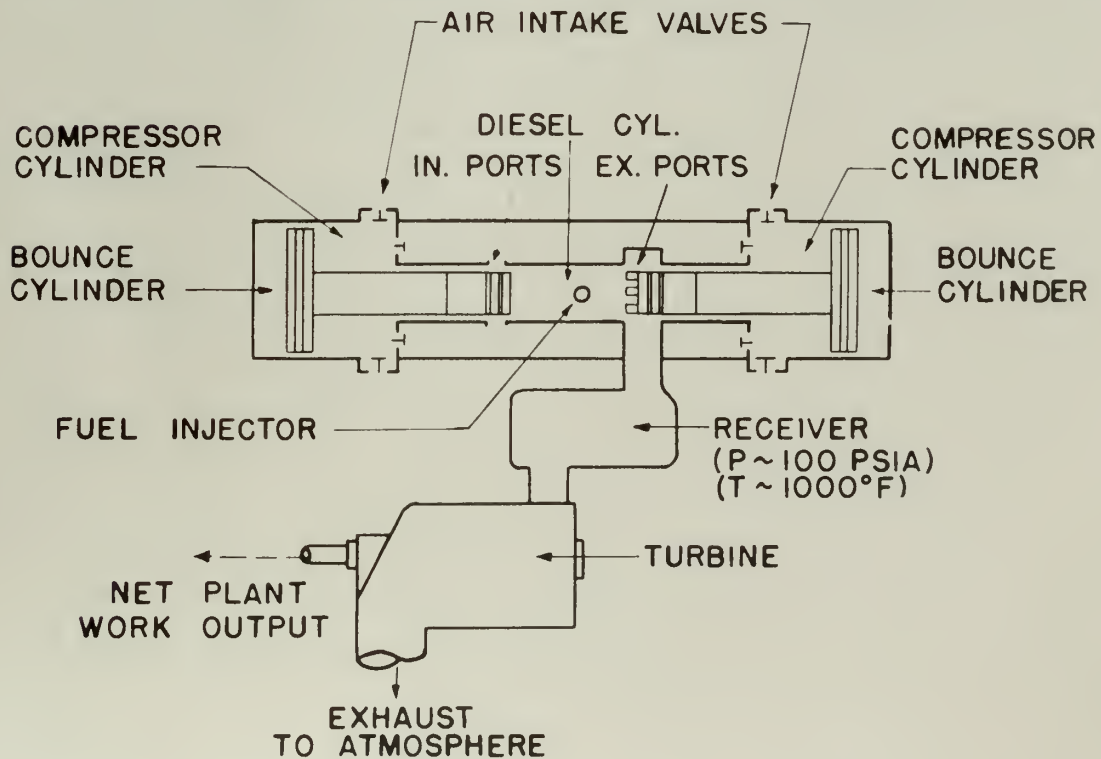
2. Characteristics of the Free-Piston Engine System.

The free-piston engine system consists of an opposed piston, supercharged two-stroke Diesel engine driving a reciprocating air-compressor and may be combined with a turbine which utilizes the expansion of the exhaust gases down to an atmospheric condition. The engine reciprocating work is directly used to provide the compressor work requirement. The free piston system is characterized by (a) constructional simplicity due to the absence of cranks and bearings; (b) almost complete freedom from vibration provided by the crankless opposed piston design; and (c) the absence of piston-cylinder side thrust and therefore reduction of cylinder wear as introduced by crank-connecting rod systems.

As shown in Fig. 1, there are two basic applications of the free-piston system. Fig. 1 (a) represents an internal-combustion engine air compressor combination (free-piston air compressor) in which the useful output is compressed air for pneumatic purposes. Fig. 1 (b) shows an air compressor internal combustion-engine combination (free-piston gas generator or gasifier) for the production of hot gases under pressure. The gasifier illustrated has an inboard compression, outboard bounce, and common central combustion chamber. Useful shaft work is derived from the hot pressurized gas by expansion to atmospheric pressure through a turbine. This investigation involved the latter configuration, i.e., the free piston gas generator or gasifier.



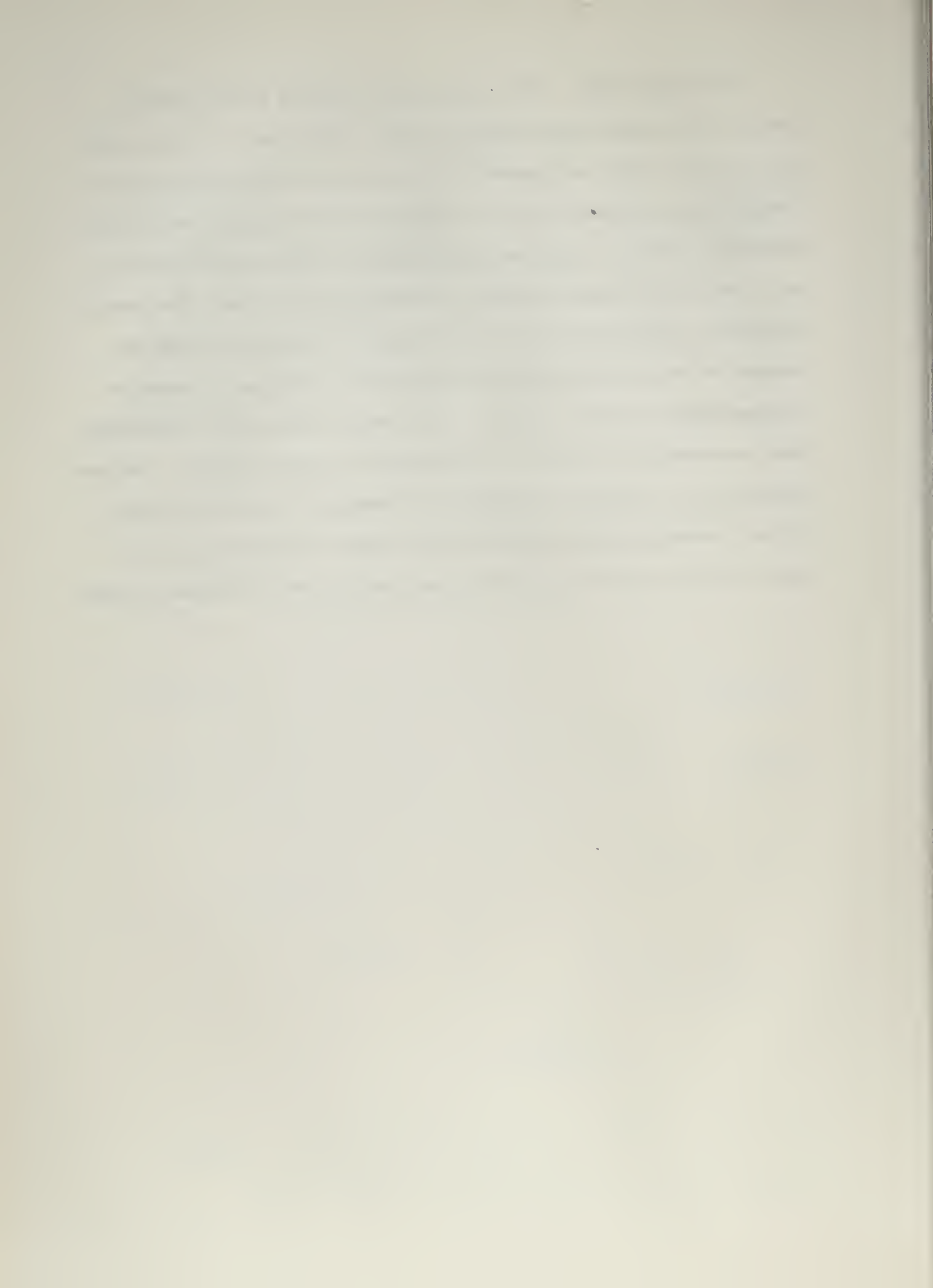
(a). FREE - PISTON COMPRESSOR SYSTEM.



(b). FREE - PISTON GAS GENERATOR-TURBINE SYSTEM.

Figure 1. Basic Applications of the Free-Piston System.

Referring to Fig. 1 (b), the gasifier consists of two opposed pistons having equal and symmetric strokes. The Diesel or power cylinder is in the center and operates as a two-stroke Diesel engine supercharged to a pressure of several atmospheres (according to turbine load condition). The two single-acting compressor cylinders are located on both ends of the central housing or scavenge air receiver. The cushion or bounce cylinders which store the energy for the return stroke are located at the outboard ends of the gasifier. Fresh air is taken in at atmospheric pressure through the air intake valves and is discharged into the scavenge air receiver surrounding the power cylinder. This compressed air is used for scavenging and charging of the power cylinder. The hot combustion gases, mixed with the excess scavenging air, exhaust into the receiver and produce the useful power in the gas turbine.



3. Dynamics of Piston Motion.

In the free-piston engine, the absence of a crank results in a "spring-mass" system which operates at a natural frequency depending on the mass of the piston assemblies and the nature of the nonlinear "gas springs" within the cylinders. London's [2] spring-mass analog for the free-piston gas generator configuration is shown diagrammatically in Fig. 2 below:

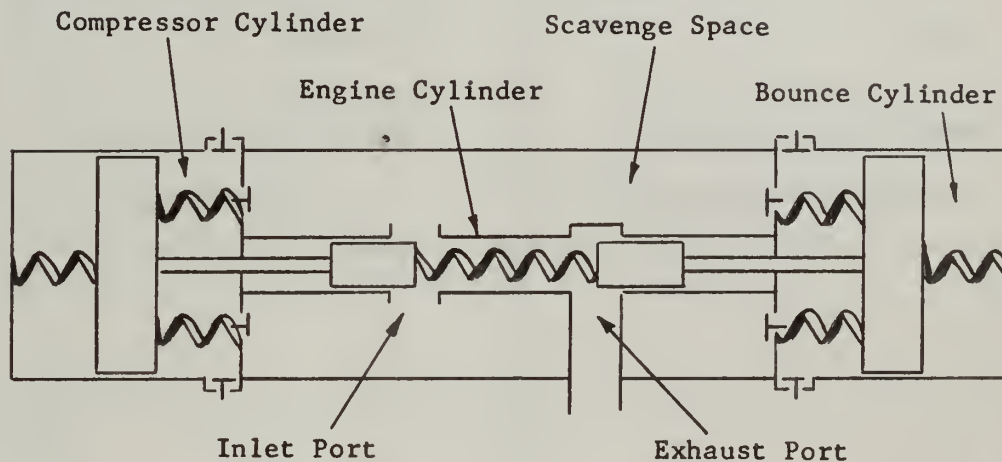


Figure 2. Spring-Mass Analog for Free-Piston Gas-Generator System.

Pressure or force versus volume or displacement diagrams for the power, compressor and bounce cylinders corresponding to the nonlinear spring forces of Fig. 2 are shown in Fig. 3. The pressure volume diagram of the power cylinder is representative of the Diesel cycle which was employed in this investigation. Also shown in this figure is a constant friction force that is independent of piston speed and gas pressures. Justification for this assumption may be found in Bobrowsky [7].

During the outward stroke of the pistons the energy produced in the power or engine cylinder in addition to that of re-expansion of

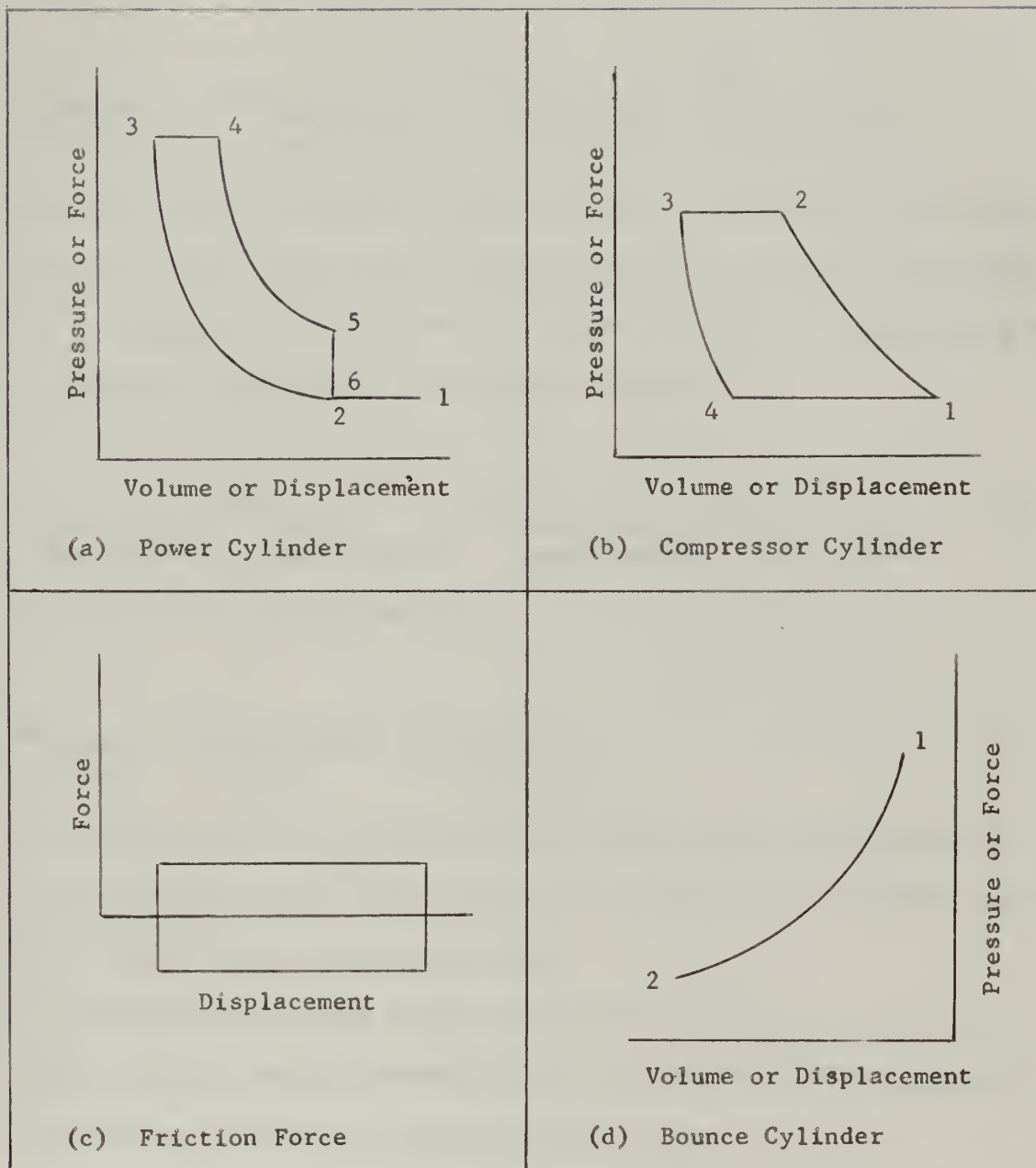


Figure 3. Forces Acting on the Free Piston.

air in the clearance space of the compressor cylinders less friction losses is stored in the cushion or bounce cylinders,

$$Wk_{\text{engine exp stroke}} = Wk_{\text{bounce cyl compr stroke}} - Wk_{\text{compressor exp stroke}} + Wk_{\text{friction per stroke}} \quad .3.1$$

During the inward stroke the energy stored in the bounce cylinders is returned to the system again discounting friction losses, compressing and discharging the air in the compressor cylinders and compressing the air used for combustion in the power cylinder,

$$Wk_{\text{bounce cyl exp stroke}} = Wk_{\text{engine compr stroke}} + Wk_{\text{compressor compr stroke}} + Wk_{\text{friction per stroke}} \quad . 3.2$$

On a net work per cycle basis,

$$Wk_{\text{engine cycle}} = Wk_{\text{compressor cycle}} + Wk_{\text{friction per cycle}} \quad 3.3$$

For each half cycle the component work terms must balance since the kinetic energy in the piston mass is zero at the inner and outer dead points where piston velocity is zero.

Newton's Second Law relates piston resultant force F_R and the piston rate of change of momentum where the resultant force F_R may be evaluated as a function of piston position from

$$\begin{aligned} F_R \text{ (out stroke)} &= F_{\text{eng}} + F_{\text{compr}} - F_{\text{bounce}} - F_{\text{fr}} \\ F_R \text{ (in stroke)} &= F_{\text{bounce}} - F_{\text{compr}} - F_{\text{eng}} - F_{\text{fr}} \end{aligned} \quad 3.4$$

The work done by the resultant force acting on the piston is equal to the gain of kinetic energy of the piston.

4. General Electronic Analog of the Free-Piston Gas Generator.

In the previous section it was shown that the free-piston engine may be considered as a "spring-mass" system with a single degree of freedom wherein the nonlinear "gas spring" forces are of a thermodynamic nature. A constant static friction force opposing piston motion is also present. As previously developed in Plow [1], the differential equation of motion of the piston in a gas generator is a mathematical expression of Newton's Second Law (Force = mass x acceleration) and is given by

$$F_e(x, \dot{x}) + F_c(x, \dot{x}) - F_b(x, \dot{x}) - F_{fr}(\dot{x}) = M\ddot{x}, \quad 4.1$$

where M is the piston mass

- $F_e(x, \dot{x})$ is the engine cylinder force on the piston
- $F_c(x, \dot{x})$ is the compressor cylinder force on the piston
- $F_b(x, \dot{x})$ is the bounce cylinder force on the piston
- $F_{fr}(\dot{x})$ is the friction force
- x is the piston displacement
- \dot{x} is the piston velocity
- \ddot{x} is the piston acceleration

It will be seen in later sections that the differential equations from which the engine, compressor and bounce cylinder forces or pressures are obtained are functions of piston displacement and velocity and that the friction force is dependent on piston velocity. Diagrams illustrating the "gas spring" and friction forces acting on the piston are shown in Fig. 3.

The electronic analog computing arrangement (from Plow [1]) for the

solution of equation 4.1 is shown in Fig. 4. The circuitry of the blocks representing the engine, compressor, bounce and friction analogs will be described in detail in following sections. Useful results from the computing arrangement of Fig. 4 for determination of gas generator performance data will consist of piston displacement as a function of time and pressure-displacement diagrams for the engine, compressor, and bounce cylinders. Pressures and displacements will appear in terms of scaled voltages.

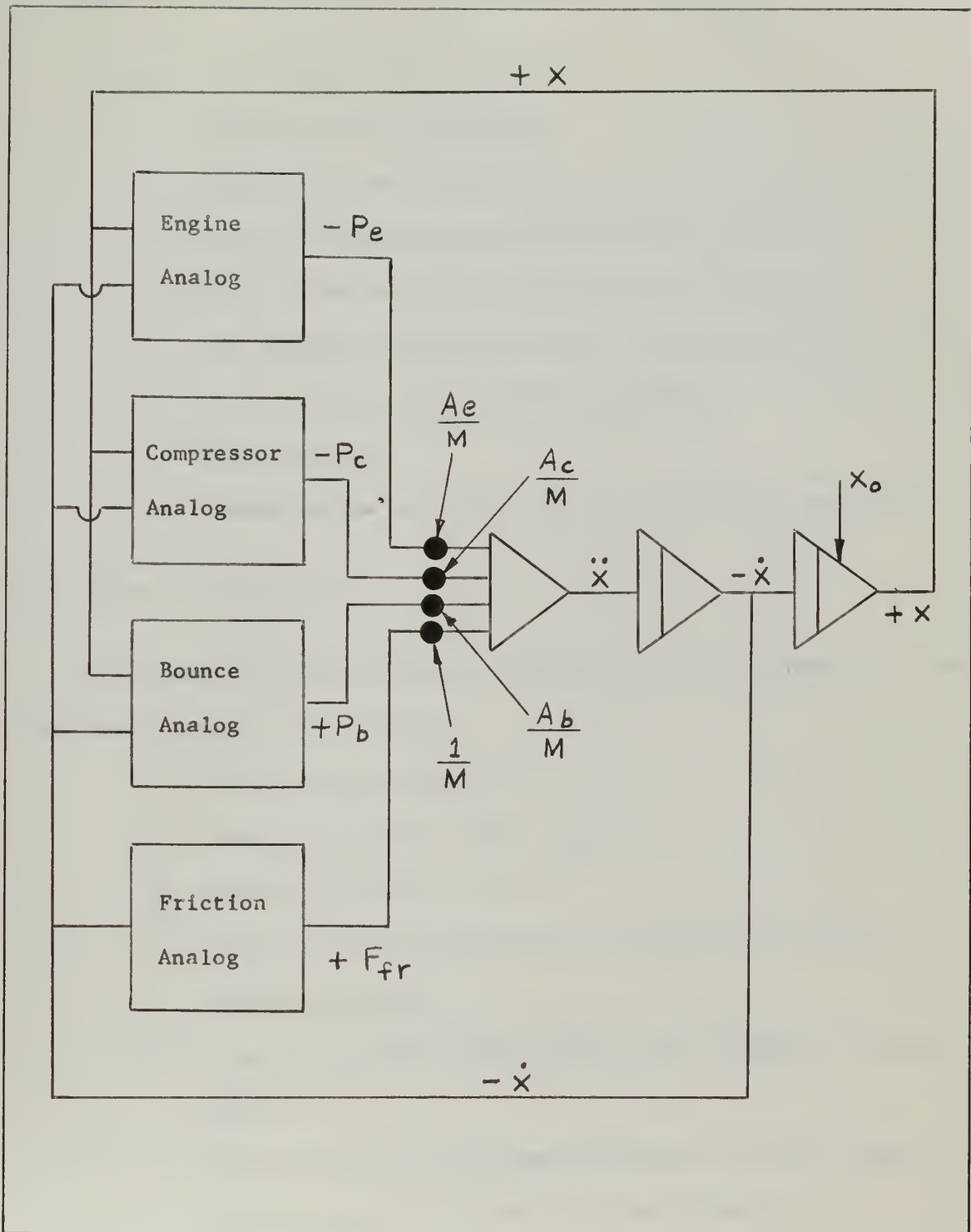


Figure 4. Basic Electronic Analog Computer Arrangement for Free-Piston Gas Generator.

5. System Inputs, Parameters, and Performance Relations.

Inputs to the system will consist of:

1. Fixed geometric parameters.
2. Initial piston displacement position (at outer dead point)
3. Various cylinder pressure conditions, which are:
 - a. Compressor intake and delivery pressures.
 - b. Engine pressure at start of compression.
 - c. Initial bounce cylinder pressure.
4. Fuel quantity.
5. Thermodynamic parameters such as polytropic exponents.

5.1 Geometric parameters.

Variables and fixed quantities depending upon the geometry of the free-piston system are as follows:

1. Engine piston area, A_e .
2. Compressor piston area, A_c .
3. Bounce piston area, A_b .
4. Engine piston displacement from midpoint or point of contact of pistons, x .
5. Compressor piston displacement from compressor cylinder head, y .
6. Bounce piston displacement from bounce cylinder head, z .
7. Engine piston displacement at port closure, x_p .
8. Piston mass, M .

The following relations also hold for the above parameters:

$$A_b = A_e + A_c, \quad 5.1.1$$

$$y = x + c, \quad 5.1.2$$

$$z = b - x, \quad 5.1.3$$

and
$$\frac{dx}{dt} = \frac{dy}{dt} = -\frac{dz}{dt} \quad 5.1.4$$

The quantities c and b in the above equations represent the clearances of the compressor and bounce cylinders respectively when the pistons are in contact at the midpoint or center of the machine. Fig. 5 below shows these relations for one-half of the gas generator configuration.

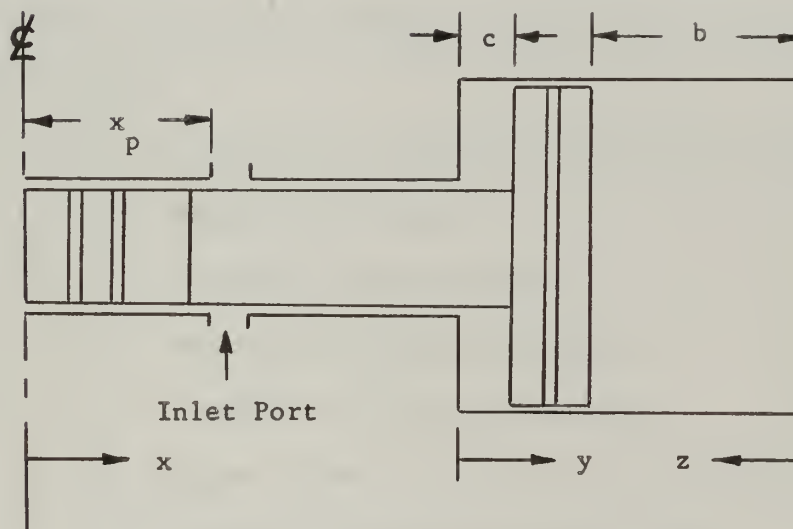


Figure 5. Illustration of Displacement and Clearance Parameters for Pistons in Contact at Midpoint.

5.2 Pressures.

In the free-piston gas generator ambient air of about one atmosphere is compressed in the compressor to several atmospheres absolute pressure depending on turbine load condition and is delivered to

the scavenge air receiver during the inward stroke of the pistons.

During the latter part of the power or outward stroke and commencement of inward stroke of the pistons, when both the exhaust ports and the intake or scavenging ports are open, the scavenging air flows through the scavenge ports and through the full length of the power cylinder, forcing the exhaust gases through the exhaust ports and into the turbine inlet receiver (See Fig. 1). Some of the scavenging air follows the exhaust gases into the receiver for good scavenging, but a portion of this supercharge air remains within the power cylinder and is compressed for the next combustion cycle during the inward stroke of the piston. Intake of fresh air into the compressor cylinders occurs during the outward piston stroke.

The significant pressures in the free piston system are thus:

1. P_o - ambient air pressure.
2. P_i - compressor intake pressure.
3. P_d - compressor discharge pressure.
4. P_s - scavenge air receiver pressure.
5. P_p - engine cylinder pressure during scavenging.
6. P_t - operating pressure at turbine inlet.

Valve pressure drop allowances of five percent of upstream absolute pressure were arbitrarily chosen for each port passage of the gas generator. These include the compressor intake and discharge valves and the engine scavenge and exhaust ports. The ratio of downstream to upstream pressure (absolute) for the compressor valves and engine ports is therefore equal to 0.95.

5.3 Temperatures

As will be seen in succeeding subsections, the significant temperatures in the free-piston problem for the determination of the masses of engine intake air, m_e , and compressor air, m_d , and for the determination of generator gas delivery temperature, T_t , are as follows:

1. Ambient air temperature, T_o .
2. Engine intake air temperature, T_p , assumed equal to compressor discharge temperature, T_d .
3. Engine exhaust gas temperature, T_e .

5.4 Masses of Engine Intake Air and Compressor Discharge Air.

Gas generator performance characteristics require the determination of engine intake and compressor discharge air masses.

Employing the equation of state of a perfect gas, the mass of engine intake air m_e , will be

$$m_e = \frac{P_p V_p}{R T_p} , \quad 5.4.1$$

where V_p is the engine cylinder volume at the point of port closure and R the gas constant for air ($R = 53.3 \text{ ft-lbf/lbm} - ^\circ\text{R}$).

Assuming engine intake air temperature, T_p , equal to compressor discharge temperature, T_d , and considering compression and expansion processes in the various cylinders to be polytropic then

$$m_e = \frac{P_p V_p}{R T_o \left(\frac{P_d}{P_i} \right)^{\frac{n_c - 1}{n_c}}} , \quad 5.4.2$$

where n_c is the polytropic compression exponent in the compressor.

Again employing the equation of state of a perfect gas, the mass of air delivered by the compressor per cylinder per cycle, m_d , is given by

$$m_d = \frac{P_i A_c Y_i}{R T_o}, \quad 5.4.4$$

where A_c is the area of the compressor cylinder and Y_i is the length of the air intake portion of the compressor stroke.

The above expressions for engine intake and compressor discharge air masses involve only one-half of the free-piston gas generator and would have to be doubled to obtain total masses for both cylinders or sides of the system.

5.5 Power Output of the System.

In the actual free-piston gasifier-turbine combination hot combustion gases mixed with excess scavenging air exhaust from the gas generator into the turbine receiver and then flow through the gas turbine which alone produces useful power. The thermodynamic state of the gases at the turbine inlet is dependent on the pressure and temperature of the exhaust gases. The product of the isentropic available energy and the gas flow rate results in the rate at which work can be obtained from the exhaust gases. By multiplying this quantity by the turbine isentropic efficiency the effective power output at the turbine shaft finally can be determined.

The exhaust gas temperature of a reciprocating internal combustion engine system is substantially less than the working substance temperature at the end of the power stroke. London [2] considers the engine

exhaust gas temperature equal to the mass average temperature of the "blow-down" period and has derived the following idealized engine exhaust gas temperature equation for a constant cylinder volume exhaust,

$$T_e = \frac{T_5}{k} \left[1 + (k-1) \frac{P_6}{P_5} \right]. \quad 5.5.1$$

Subscripts 5 and 6 represent the state points at beginning and end of exhaust or "blow-down" period (See Fig. 3). Temperature at state 5 is determined from the equation of state of a perfect gas,

$$T_5 = \frac{P_5 V_5}{m_e R}, \quad 5.5.2$$

where m_e is mass of engine intake air as obtained from equation 5.4.1 and R is the gas constant for air.

The generator gas delivery temperature, T_t , is then equal to the mass average between engine exhaust gas temperature, T_e , and scavenge gas or engine intake air temperature, T_p , and is given by,

$$T_t = \frac{m_e}{m_d} T_e + \left(1 - \frac{m_e}{m_d} \right) T_p, \quad 5.5.3$$

where m_e/m_d is the ratio of engine air to compressed air delivered, m_e and m_d being obtained from equations 5.4.1 and 5.4.4 respectively, and T_p assumed equal to compressor discharge temperature, T_d , is obtained from

$$T_p = T_d = T_o \left(\frac{P_d}{P_i} \right)^{n_c - \frac{1}{n_c}}, \quad 5.5.4$$

with quantities as defined in preceding subsections.

With the working substance considered a perfect gas, due to relatively low delivery pressures of the free piston gasifier, enthalpy of exhaust gases may be considered a function of temperature alone and isentropic available energy determined. The power out of the gas turbine is the product of the isentropic available energy, total exhaust gas flow rate considering the two sides of the gas-generator, and turbine isentropic efficiency. Including appropriate conversion factors, the equation representing power output in horsepower is given by,

$$(\text{shp})_{\text{turbine}} = \frac{(\Delta h_s)(778)(2)(m_d)(f_r)(\eta_t)}{33,000}, \quad 5.5.5$$

where Δh_s is the isentropic available energy (Btu/lbm),

m_d is the mass (lbm) of air delivered by the compressor per cylinder per cycle,

f_r is the piston frequency in cycles per minute,

and η_t is the turbine isentropic efficiency.

6. Electronic Analog of the Two-Stroke Standard Diesel Cycle.

Fig. 3(a) shows a representative pressure versus volume indicator diagram for the two-stroke air standard Diesel cycle assumed in this investigation. With the absence of a crank mechanism in the free-piston gas generator, the stroke of the system and hence the engine compression ratio and compressor and bounce cylinder clearance volumes are all variable quantities dependent on the load conditions. The only fixed geometrical point for the piston in the engine cylinder is that of port closure. The thermodynamic state of the engine intake air mass at this point can be determined for a given compressor discharge pressure which is also dependent on load conditions.

As previously considered, the working substances in all the cylinders of the free-piston system are assumed to be perfect gases and compression and expansion processes polytropic. Again referring to the indicator diagram of Fig. 3(a), the two-stroke standard Diesel cycle can be seen to consist of the following processes:

1. Polytropic compression, at exponent n_e , of engine charge after port closure.
2. Injection and burning of fuel to give addition of energy at constant pressure during first portion of power stroke.
3. Polytropic expansion, at exponent n_e' , of engine charge and products of combustion.
4. Engine "blow-down" of exhaust gases at constant volume.
5. Scavenging at constant pressure.

For a polytropic process involving a perfect gas

$$PV^n = \text{constant}, \quad 6.1$$

where n is the polytropic exponent. By differentiation and considering time as the independent variable, we obtain

$$\frac{dP}{dt} = - \frac{n P \frac{dv}{dt}}{V} \quad 6.2$$

With the volume given by

$$V = A_e x, \quad 6.3$$

and

$$\frac{dv}{dt} = A_e \frac{dx}{dt} = A_e \dot{x}, \quad 6.4$$

then equation 6.2 becomes

$$\frac{dP}{dt} = - \frac{n P \dot{x}}{x} \quad 6.5$$

Following the procedure in Plow [1], the above two-stroke standard Diesel cycle processes can be defined in terms of equation 6.5 as follows.

1. Compression process.

$$\left(\frac{dP_e}{dt}\right)_{n_e} = - \frac{n_e P_e \dot{x}}{x} \quad 6.6$$

2. Combustion process.

$$\left(\frac{dP_e}{dt}\right)_P = 0. \quad 6.7$$

3. Expansion process.

$$\left(\frac{dP_e}{dt}\right)_{n'_e} = - \frac{n'_e P_e \dot{x}}{x} \quad 6.8$$

P_e in the above equation is engine cylinder pressure.

The electronic analog of the compression or expansion processes as represented by equations 6.6 and 6.8 is as follows:

1. Integrate $\frac{dP_e}{dt}$ to obtain $-P_e$ with an appropriate initial condition, P_p .
2. Multiply $-P_e$ by $n_e \dot{x}$ or $n_e' \dot{x}$ to give $-n_e P_e \dot{x}$ or $-n_e' P_e \dot{x}$ as appropriate.
3. Divide by x resulting in the formation of equation 6.6 or 6.8 and thus returning to the starting point of the analog circuit loop.

The analog of the Diesel cycle applying the above processes and procedure is shown schematically in Fig. 6. Also shown is the modification of the circuit of Plow [1] employing single quadrant electronic multiplication for more uniform and stable operation. In this investigation single quadrant multiplication was employed in each of the circuits simulating engine, compressor and bounce cylinder pressures. This was accomplished through the use of additional switching relays and sign changing amplifiers in order that the electronic multipliers (BEM and DEM)¹ involved in each of these circuits would function only in one quadrant.

A detailed explanation of the circuit of Fig. 6 follows:

1. The relay switch in the feedback of Amplifier 1 is closed whenever x is greater than x_p establishing the initial condition, P_p .
2. The electronic multiplier and its associated amplifier, Amplifier 2, together give a product of one-fiftieth of the variable inputs to the multiplier.

¹Circuit component symbols defined in Appendix IV.

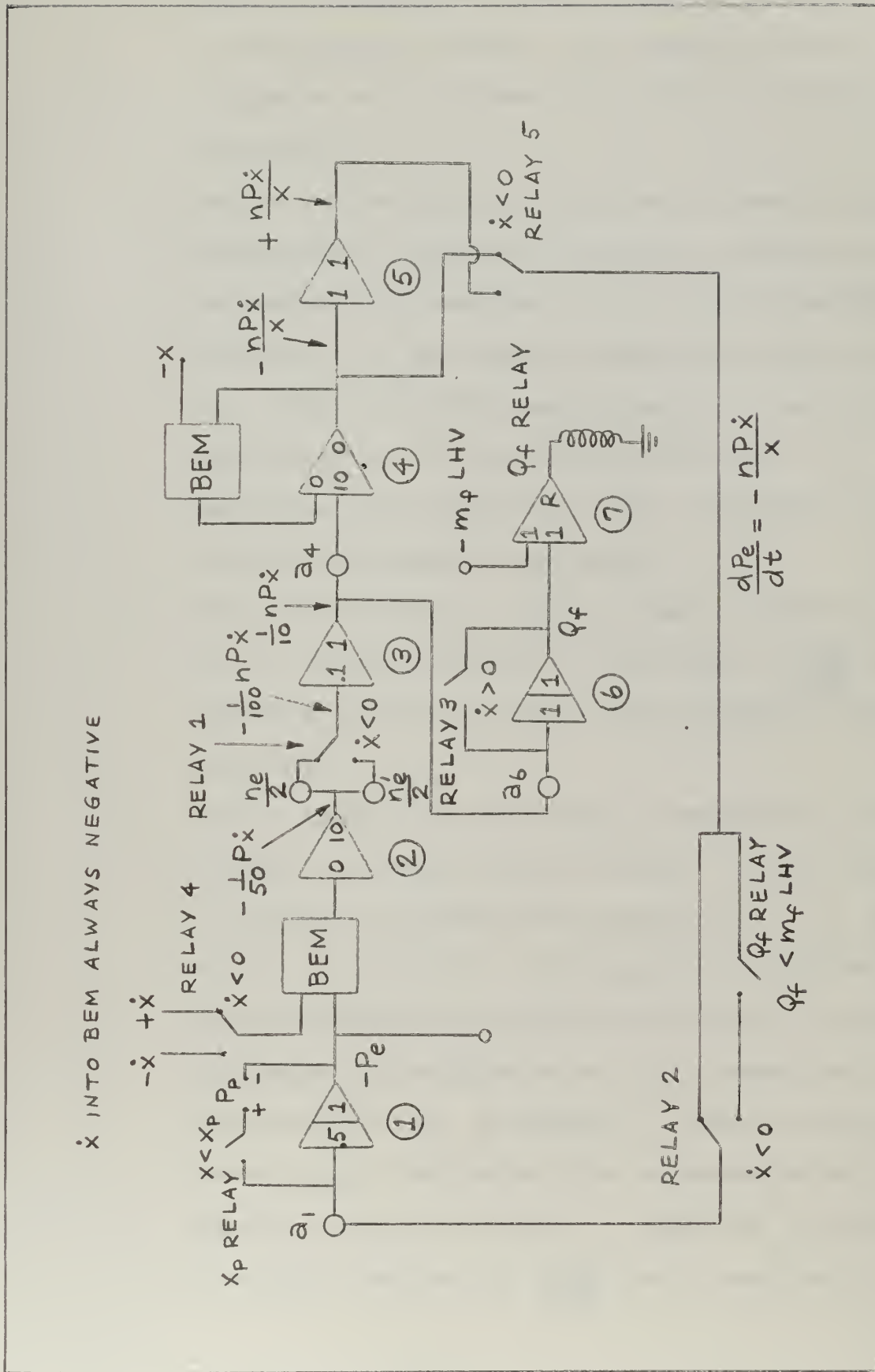
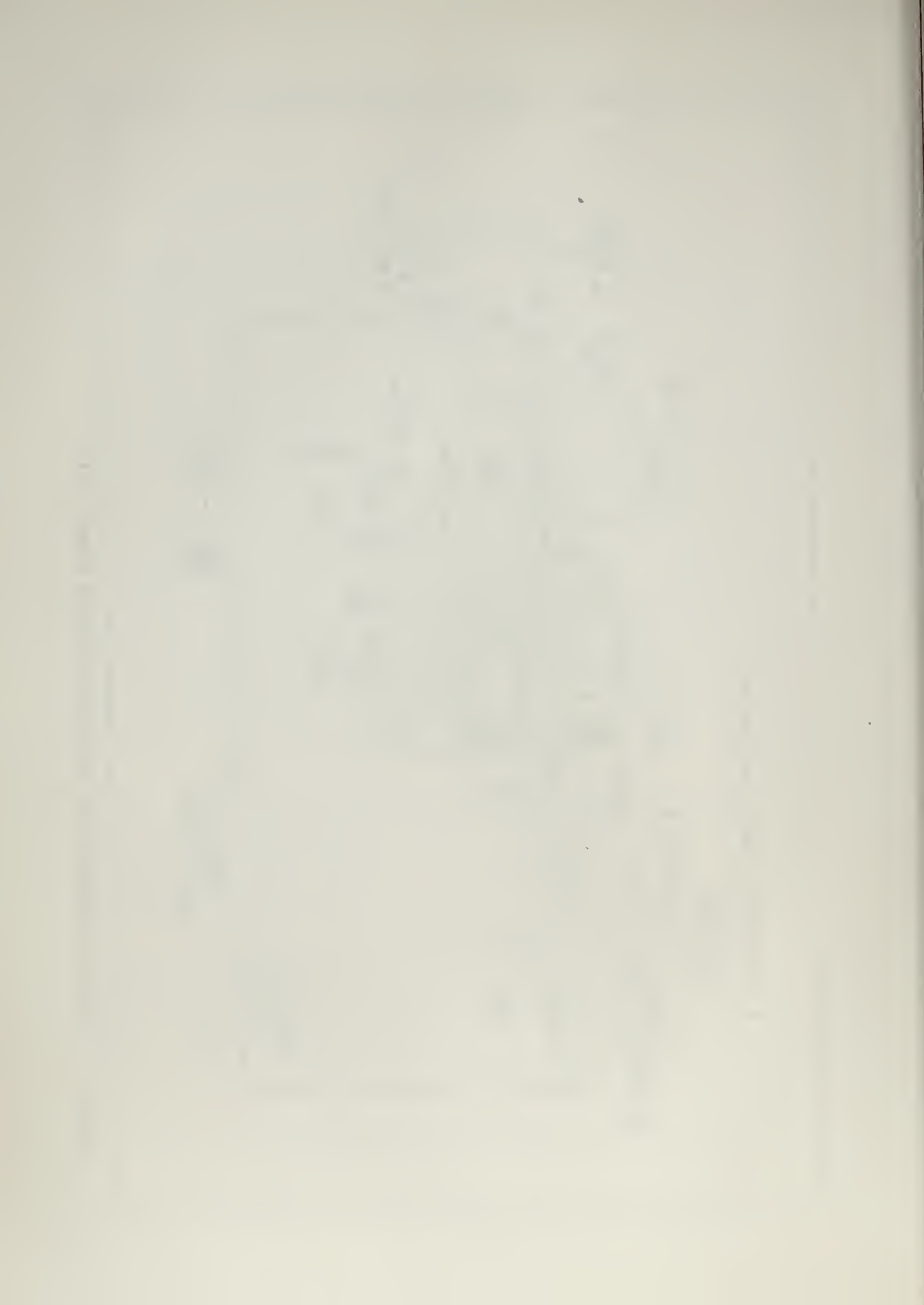


Figure 6. Electronic Analog of the Two-Stroke Standard Diesel Cycle.



3. Relay 1 is actuated by a change in sign of velocity, \dot{x} , and applies the exponent $n_e/2$ when the velocity is negative and the exponent $n_e'/2$ when the velocity is positive.
4. Division of a variable by another variable quantity is accomplished by connecting an electronic multiplier in the feedback of an amplifier as in the case of Amplifier 4. The divisor, $-x$, must always be negative for stable operation, while the variable input to Amplifier 4 may have either polarity. The coefficient potentiometer, a_4 , in conjunction with the dividing network, is adjusted to give ten times the quotient of the inputs.
5. Relay 2 is actuated by a change in sign of velocity, \dot{x} , and in conjunction with the Q_f relay makes $\frac{dP_e}{dt} = 0$ simulating injection of fuel at the commencement of the power stroke.
6. Relay 3, connected in the feedback of Amplifier 6, is also actuated by a change in sign of velocity, \dot{x} , and results in Amplifier 6 performing the integration of $-\frac{1}{10} n_e' P \dot{x}$ whenever \dot{x} is positive. The integration of this quantity produces a result which is proportional to the total instantaneous fuel energy which in turn is compared with the desired value of Q_f in Amplifier 7. When the fuel energy becomes equal to the desired value as represented by a negative voltage corresponding to $m_f LHV$, the Q_f relay is actuated, reconnecting $\frac{dP_e}{dt}$ back to Amplifier 1

through Relay 2. This action terminates fuel input and initiates the polytropic expansion process.

7. The action of Relays 4 and 5 is to enable the use of single quadrant multiplication in the circuit. These relays are both actuated by a change in sign of velocity, \dot{x} . Relay 4 is so actuated that the input, \dot{x} , to the electronic multiplier is always negative in sign. Relay 5 and Amplifier 5 are therefore required and so connected to obtain the proper polarity feedback to Amplifier 1 for each stroke.

7. Electronic Analog of the Reciprocating Compressor.

A typical pressure versus volume indicator diagram for a reciprocating compressor is represented by Fig. 3(b). The cycle is considered to consist of polytropic compression and expansion of air at exponent n_c and constant pressure air intake and discharge.

The computing arrangement for solution of the polytropic equation for the compressor,

$$\frac{dP_c}{dt} = - \frac{n_c P_c \dot{y}}{y}, \quad 7.1$$

is similar to that of the engine cycle. However, in this case diode limiters are employed on the amplifier generating P_c to establish limiting voltages corresponding to the intake and discharge pressures. This is in conformance with the circuit developed in Plow [1] with the exception that single quadrant electronic multiplication was again employed involving the necessary two extra switching relays and additional sign changing amplifier.

A schematic diagram of the compressor analog with the single quadrant multiplication feature is shown in Fig. 7. The various functions of the circuit components in performing the polytropic compression and expansion processes are essentially the same as those described for the engine analog in the preceding section.

\dot{y} INTO DEM ALWAYS NEGATIVE

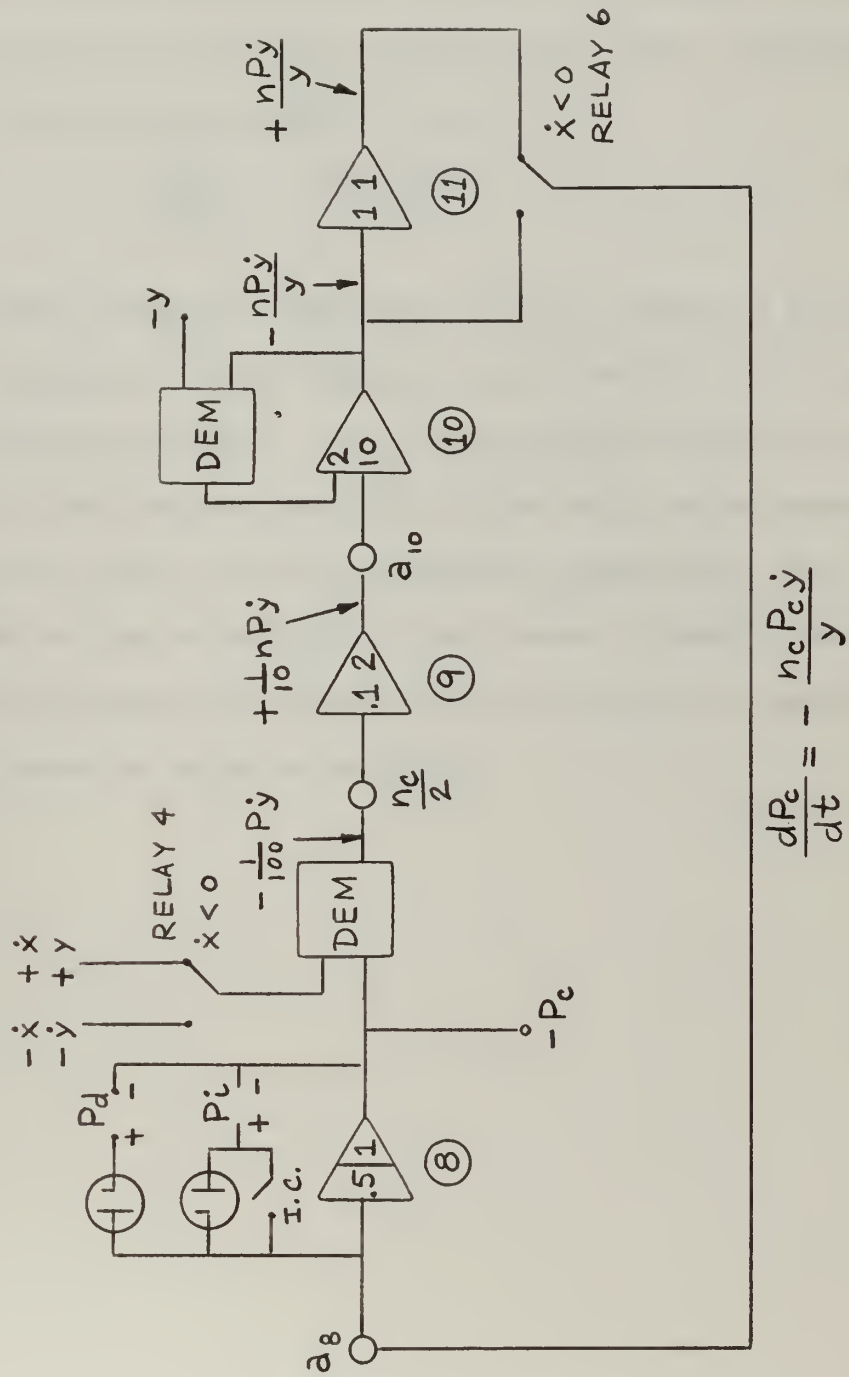


Figure 7. Electronic Analog of the Reciprocating Compressor.

E. Electronic Analog of the Bounce Cylinder "Gas Spring".

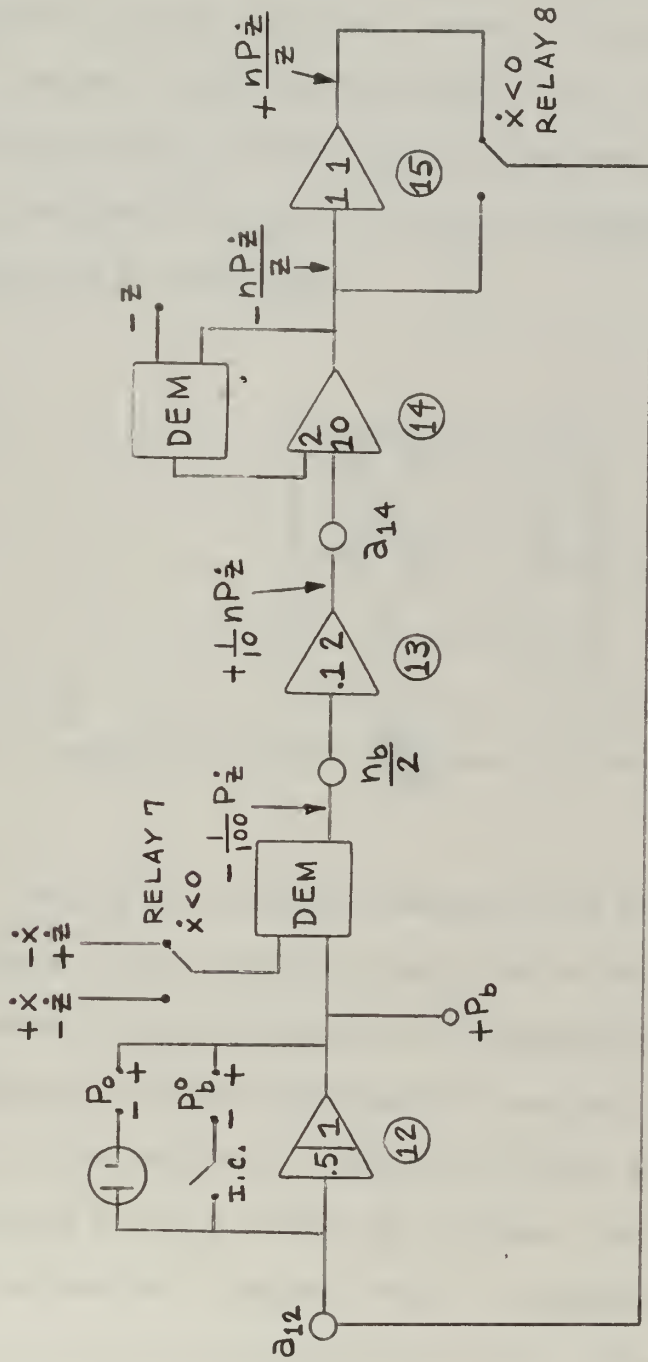
For the bounce cylinder analog, air is alternately expanded and compressed by reversible polytropic processes at exponent n_b resulting in a pressure-volume diagram as shown in Fig. 3(d). The differential equation involved for the computing loop is

$$\frac{dP_b}{dt} = - \frac{n_b P_b \dot{z}}{z}, \quad 8.1$$

and the schematic diagram of the analog circuit is shown in Fig. 8.

The employment of single quadrant multiplication in this circuit had its most advantageous effect. In the corresponding circuit of Plow [1] the absence of this feature resulted in errors which became magnified with time by the lack of an initial condition imposed each cycle. This modification resulted in stability of the bounce cylinder circuit or the ability of the pressure-displacement curve to reproduce or retrace itself over a number of cycles of operation.

\dot{z} INTO DEM ALWAYS POSITIVE



$$-\frac{dP_b}{dt} = +\frac{nbP_b\dot{z}}{z}$$

Figure 8. Electronic Analog of the Bounce Cylinder "Gas Spring".

Handwritten text, possibly a page number or header, located at the top left of the page.

Handwritten text, possibly a title or section header, located in the upper middle part of the page.

Main body of handwritten text, consisting of several lines of cursive script, located in the center of the page.

Handwritten text, possibly a signature or date, located at the bottom right of the page.

9. Electronic Analog of the Friction Force.

In this investigation a coulomb friction force, "C", only was considered. This force was assumed to be independent of piston speed and gas pressures [7] and therefore constant in magnitude. An illustration of the coulomb friction force is given in Fig. 3(c).

The friction analog of Plow [1] involving both coulomb and viscous friction was modified to produce a voltage corresponding to coulomb friction alone and is shown below:

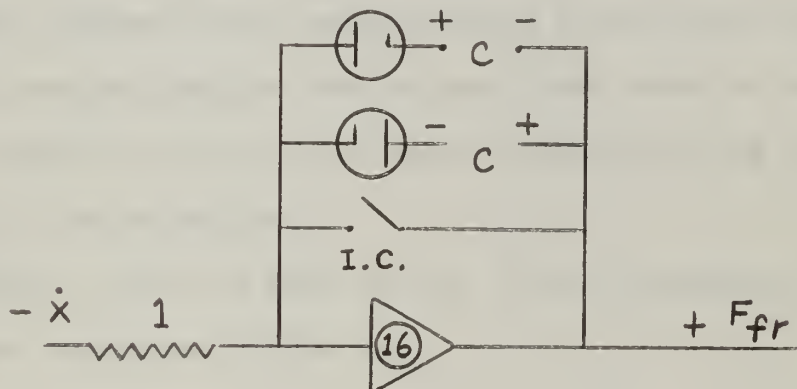


Figure 9. Electronic Analog of the Friction Force.

The limiters in the feedback of the friction analog amplifier serve the purpose of establishing the equal magnitude but opposite polarity voltages, "C", corresponding to a constant friction force, at the output of the amplifier. With this circuit, employing the negative of piston velocity voltage as the input, the appropriate output polarity voltage for a complete stroke is obtained at the instant of commencing the instroke and outstroke of the piston. Those voltages are of the proper polarity for the complete analog circuit to be shown in the following section.

10. Electronic Analog of the Free-Piston Gas Generator.

The preceding electronic analogs for simulation of the engine, compressor and bounce cylinder and friction forces were individually assembled and tested using the artificial stroke input circuit of Plow [1]. The artificial stroke consisted of displaced sinusoid voltages simulating piston motion at about one cycle in ten seconds based on real time. These voltages included the variable "x", "y", and "z" displacement voltages employed in the engine, compressor, and bounce cylinder analogs respectively.

On tying together these component analog circuits with additional amplifiers to sum and integrate the various piston forces to obtain its motion, the complete free-piston analog was obtained and the artificial stroke input no longer required.

The complete circuit is shown in Fig. 10 and corresponds to the basic computer arrangement of Fig. 4.

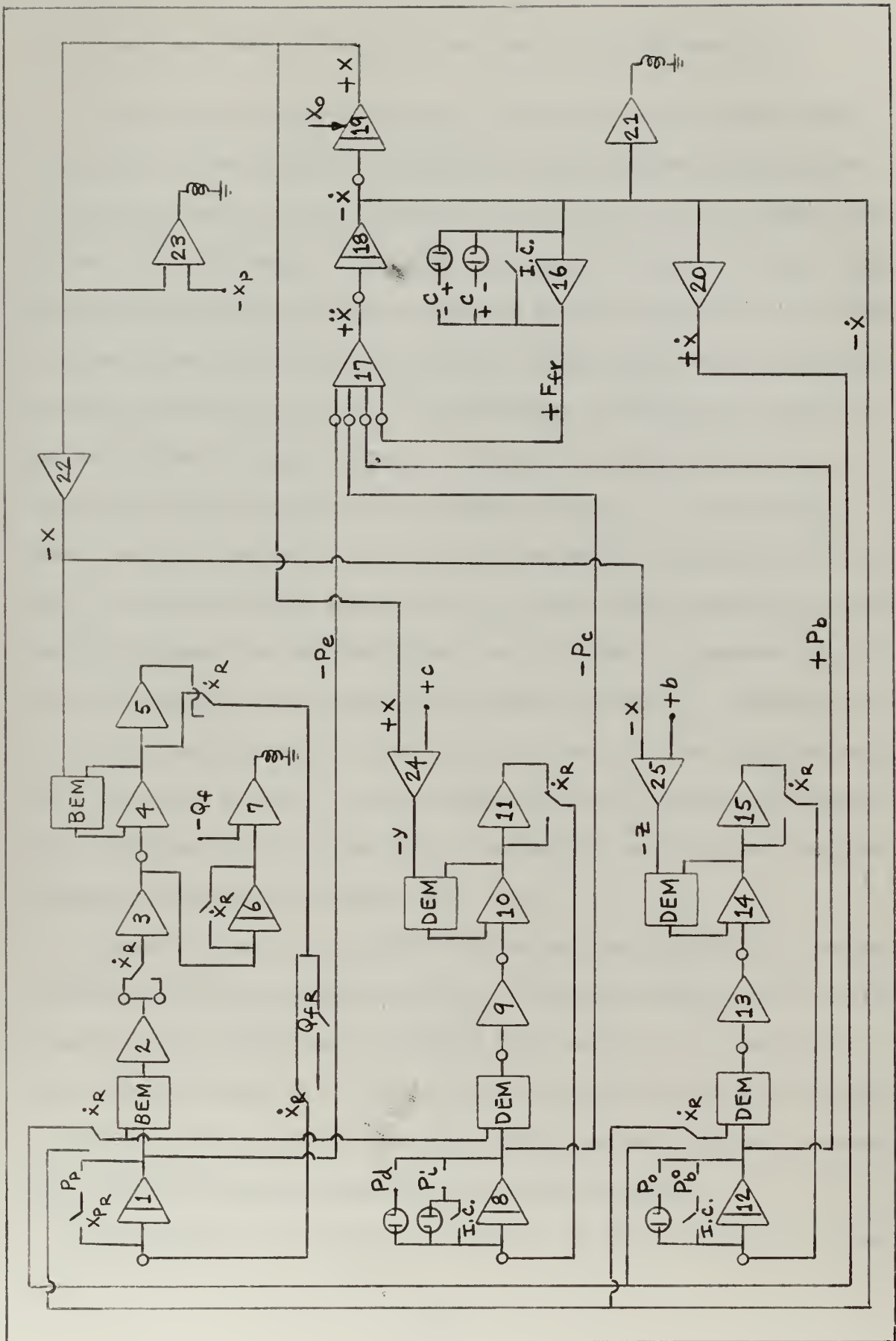


Figure 10. Electronic Analog of the Free-Piston Gas Generator.

11. Operating Characteristics of the Free-Piston Gas Generator.

In the free-piston gas generator, the omission of a crank mechanism permits a free stroke and therefore variable operating conditions of piston movement. Since there is no fixed limits for the stroke, the motion of pistons should respect certain ranges of inner and outer dead point positions, IDP and ODP, as measured from the midpoint of the engine cylinder. The limits of ODP should fall within ODP_{min} where scavenging becomes insufficient and ODP_{max} corresponding to mechanical contact at the outer limit of piston travel. IDP must lie between the point of contact of the two pistons at the midpoint ($IDP_{min} = 0$) and IDP_{max} where ignition temperature is no longer reached by compression (200 psi). IDP_{min} or clearance also should not be so small that excessive peak combustion pressures are reached in the power cylinder as compression pressure is dependent on the super-charge pressure and IDP_{min} . Operating stability of a gasifier is thus the ability to keep the piston motion within the limits just defined. For the SIGMA GS-34 gas generator the approximate operating limits for the ODP are between 16 and 20 inches from the midpoint of the engine cylinder. [5]

Changes in load on a gasifier coupled to a gas turbine are effected by adjusting the gas delivery pressure to the power demand on the turbine. In general the turbine has no throttle valve and is of a fixed nozzle area, full-admission type. The load on a gas generator then corresponds to the gas delivery pressure which is related by valve and port pressure drops to the scavenge and compressor discharge pressures.

The frequency of operation is dependent on the gas delivery or load

and on the compression pressure in the diesel cylinder. The higher these pressures are, the greater is the frequency of oscillation. The operating frequency decreases automatically with decreased load, or lower supercharge, resulting in lower air flow rate in accordance with the decreased turbine requirement. To assist in adapting the gas output to changes in turbine load, the position of the ODP is shifted, being moved inward for a decrease in power.

For each pressure level in the gas generator, a certain specific mean pressure is required in the bounce cylinders in order to obtain desired stroke lengths and compression ratios in the power and compressor cylinders. For different load conditions, the air pressure in the bounce cylinders is regulated by a device called the "stabilizer" designed so that the average pressure in the bounce cylinders is independent of the stroke and varies linearly with scavenge air pressure. Scavenge air pressure in turn is dependent on turbine load. The stabilizer therefore provides an automatic adjustment of the bounce cylinder pressure, and hence compression pressure in the engine cylinder to any imposed operating pressure. The compression pressure also may be chosen freely for each delivery pressure by proper adjustment of the bounce cylinder pressure. Full advantage of free-piston machinery is obtained through use of the stabilizer control which provides for flexible operating conditions.

In order to vary the gas load of a generator it is therefore necessary to change the amount of fuel injected and to change the bounce cylinder pressure. Bounce cylinder pressure is dependent on the operating pressure and is automatically adjusted to new load conditions as previously described.

The power output of a gasifier-turbine combination is controlled by changing the delivery pressure of the gasifier and by generating gas at the correct rate corresponding to the turbine consumption capacity. However for low power outputs of the turbine, the generator is restricted to a minimum gas flow rate which is considerably greater than turbine requirements. With reduction of fuel to the gasifier, piston frequency and stroke are reduced. This may occur until a minimum stroke is reached which must always be sufficient to uncover the ports to prevent stalling the engine. This operating point defines the "technical minimum" of the gasifier and according to BARTHALON and HORGEN [5] occurs at 25 per cent of full load for the SIGMA GS-34 gas generator. Thus if it is desired to operate a single gasifier-turbine combination at a lower output it would be necessary to by-pass the excess gas. This of course would result in a direct loss of energy and unfavorable fuel economy at low loads.

12. Simulation of Full and Part Load Performance of the SIGMA GS-34 Free-Piston Gas Generator on the Analog Computer.

In this investigation simulation of full and part load performance of a gas generator was conducted on the analog computer using the fixed geometric and variable operating parameters of the SIGMA GS-34 gasifier. The generator was assumed to be directly coupled to a gas turbine with an isentropic efficiency of 85 percent.

Simulation of full load was first performed on the computer with results of this run compared with actual performance data [2] and [4] followed by part load runs of 75, 50, and 25 percent of full load (25 percent load being so called "technical minimum"). Gas delivery pressures, P_t , for these loads were obtained from London [2] and Barthalon [6] and are as follows (refer to section 5 for system parameters):

Load Percent	Gas Delivery Pressure, P_t , (psia)
100	64.5
75	54.0
50	45.0
25	37.0

As related in the previous section, mean effective bounce cylinder pressure was considered to vary linearly with scavenge air or gas delivery pressure. Eichelberg [3] also shows essentially a constant pressure differential between maximum bounce cylinder pressure and scavenge air pressure over the entire operating load range of the SIGMA GS-34 gas generator. Thus with initial or maximum bounce cylinder pressure avail-

able for full load, [4] values of this pressure may be determined for any operating condition.

The analog computer circuit established in this investigation simulates a steady state operating condition of a gas generator and is incapable of solving a transient problem such as start up of the gasifier or a change in load condition. The initial condition for the computer problem is with the piston at the outer limit of its stroke (ODP) or initial piston displacement (x_0) and the bounce cylinder pressure at its maximum or initial value (P_b^0). A cycle of operation would involve the travel of the piston inward to the inner dead point position (IDP) and return to the initial starting point. Section 3 describes in detail the dynamics and forces involved in the piston motion.

With the computer properly programmed for simulation of a particular load as set down in detail in Appendix II the criteria for performing each run was to vary initial piston displacement position, x_0 , so that a maximum engine compression pressure of close to 1500 psia was attained at the end of the instroke and to adjust the amount of fuel input to return the stroke to the initial starting point. The figure 1500 psia was selected as a nominal value for the standard Diesel cycle employed in this investigation considering normal operating values of compression pressure for the SIGMA GS-34 gas generator. [3] The above adjustments of initial piston displacement and fuel setting had to be made while observing engine pressure versus piston displacement diagram on the recording equipment. With these adjustments properly made, two to three fairly reproducible cycles could be attained representing the steady state operating condition for the particular load run. The adjustments at the same time were

rather critical due to inherent drifts in the computer circuit components.

Comparison of analog computer solution results with actual performance data for the SIGMA GS-34 gas generator at full load condition is as follows:

	GS-34	Analog
1. Gas Turbine		
Power output, shp	1138	1290
Gas flow rate, lbm/hr	29000	39400
Gas pressure at inlet, psia	64.5	64.5 ¹
Gas Temp. at inlet, deg F abs	1405	1174
2. Gas Generator		
Frequency, cpm	613	649
Stroke, inches	17.5	18.25
Engine effective stroke, inches	9.7	10.0
Engine clearance, inches	1.29	1.0
Compressor clearance, inches	2.38	2.0
Bounce clearance, inches	8.0	7.7
Compressor air delivered, lbm/cylinder-cycle	0.388	0.507
Ratio engine/compressor air	0.47	0.404
Air-fuel ratio	32	35

¹Inputs to the computing problem included actual performance data pressures as here shown in addition to fixed geometric parameters.

	GS-34	Analog
Engine indicated thermal efficiency, LHV basis	29.8	51.3
3. Gas Generator-Turbine System		
Fuel flow rate, lbm/hr	460	452
Brake specific fuel consumption, lbm/shphr	0.404	0.351
Thermal efficiency, LHV basis	34.6	39.8

On a net work per cycle basis, engine work is equal to the sum of compressor and friction work from equation 3.3 and for the computer results at full load a discrepancy of 17.0 percent on basis of net engine work was obtained.

Figs. 11, 12, and 13 show the full load pressure versus displacement diagrams for the engine, compressor, and bounce cylinders respectively.

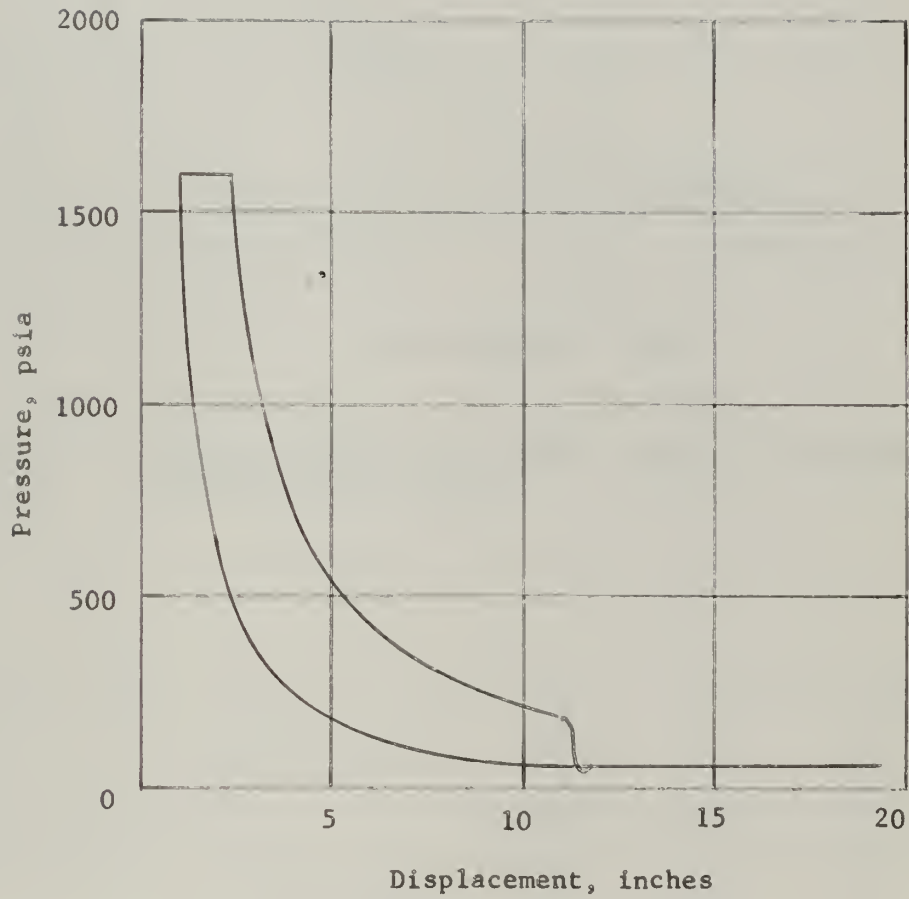


Figure 11. Pressure versus Displacement Diagram for Engine Cylinder at Full Load.

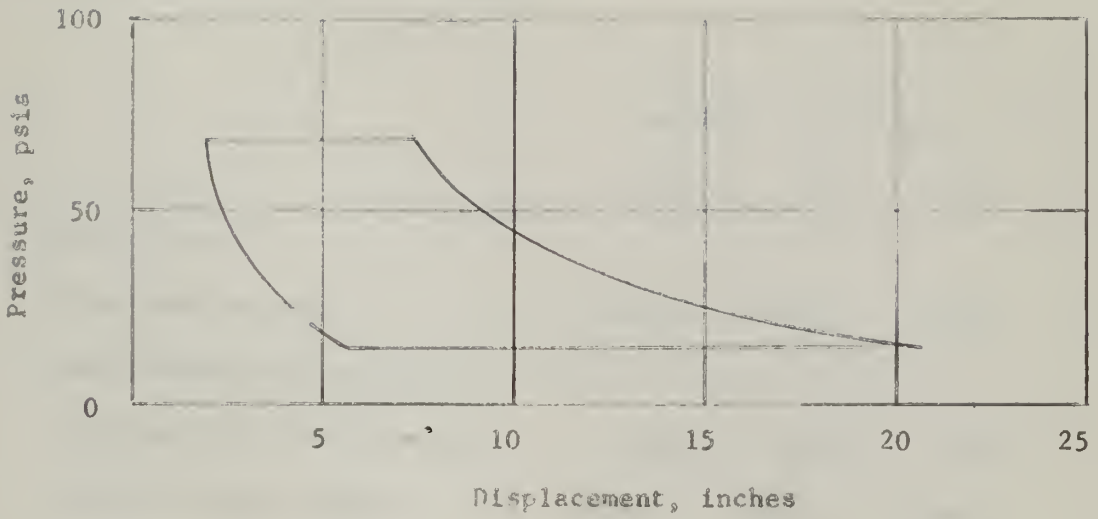


Figure 12. Pressure versus Displacement Diagram for Compressor Cylinder at Full Load.

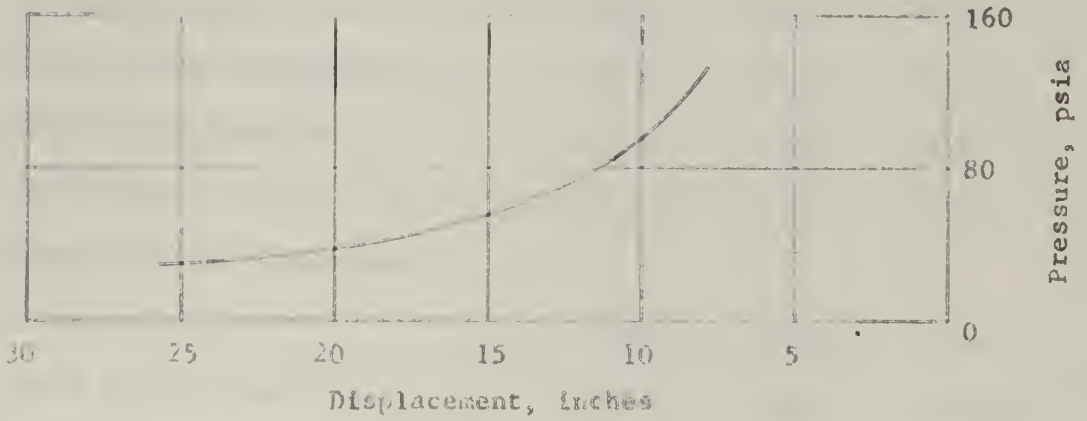


Figure 15. Pressure versus Displacement Diagram for Bounce Cylinder at Full Load.

Computer solution results for part-load performance with operating pressure varied as previously described are shown in the table below for load percentages as indicated:

	Percent of Full Load		
	75	50	25
1. Gas Turbine			
Power output, shp	963	687	442
Load percent on basis of computer full load results	74.7	53.2	34.2
Gas flow rate, lbm/hr	36100	33800	31000
Gas pressure at inlet, psia	54.0	45.0	37.0
Gas temp. at inlet, deg F abs	1066	925	767
2. Gas Generator			
Frequency, cpm	605	561	517
Stroke, inches	18.05	17.85	17.65
Engine effective stroke, in.	10.1	10.15	10.15
Engine clearance, in.	0.9	0.85	0.85
Compressor clearance, in.	2.0	1.95	1.95
Compressor air delivered, lbm/cyl-cycle	0.497	0.503	0.500
Ratio engine/comp. air	0.360	0.309	0.268
Air-fuel ratio	36.7	40.5	51.0
Engine ind. thermal eff., LHV basis	0.516	0.572	0.656

	Percent of Full Load		
	75	50	25
3. Gas Gen.-Turb. System			
Fuel flow rate, lbm/hr	354	258	163
BSFC, lbm/shphr	0.368	0.375	0.369
Thermal eff., LHV basis	38.0	37.2	34.3

Net work discrepancies between engine and sum of compressor and friction work for the part-load conditions are as follows:

Percent of Full Load	Discrepancy, percent
75	9.0
50	4.6
25	7.2

Figures 14 through 22 show pressure versus displacement diagrams of the engine, compressor, and bounce cylinders for the three part-load conditions. Figures 23 through 29 show performance characteristics for full and part-load operating conditions as obtained from the analog computer solution results. Also, shown on these graphs are the actual performance operating points for the GS-34 gasifier for full load condition.

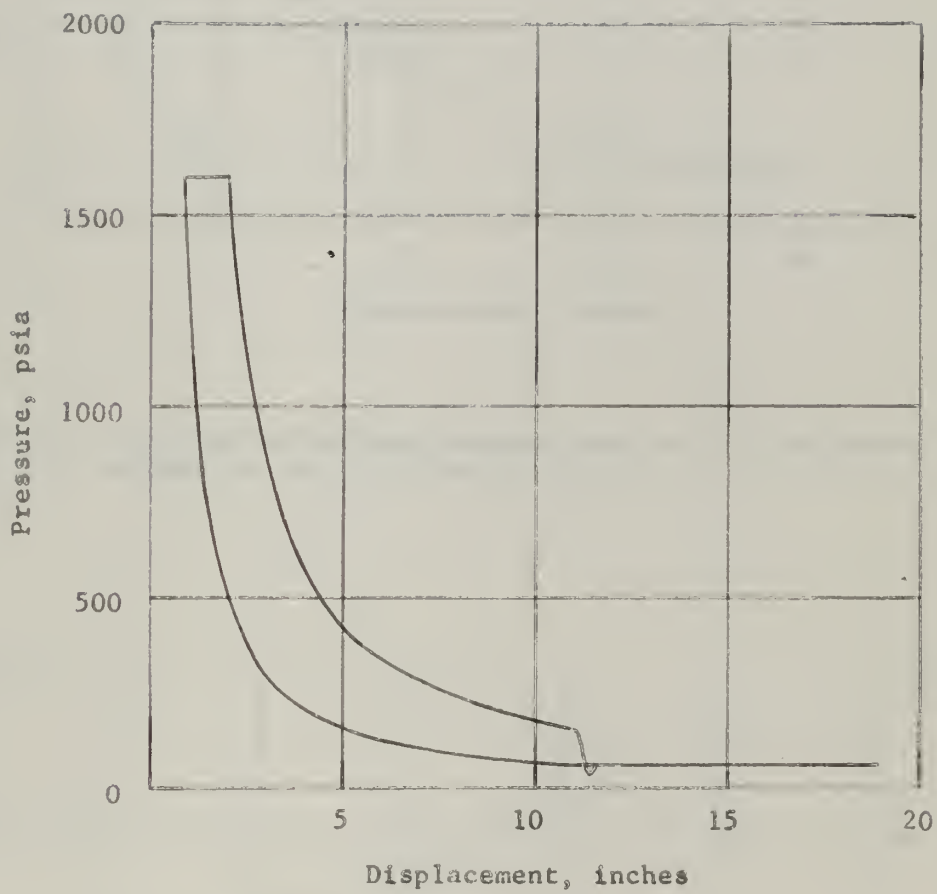


Figure 14. Pressure versus Displacement Diagram for Engine Cylinder at Three-Quarters Load.

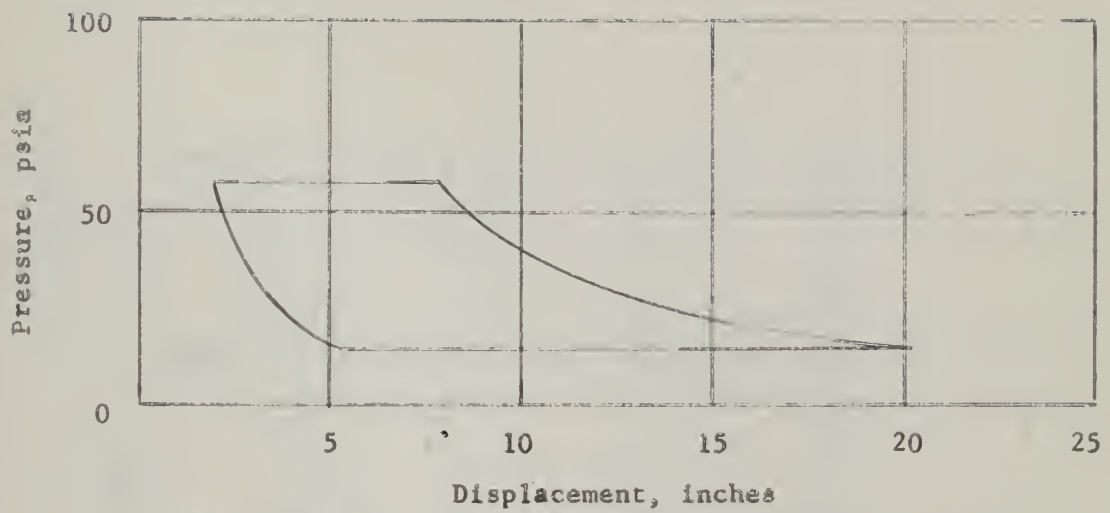


Figure 15. Pressure versus Displacement Diagram for Compressor Cylinder at Three-Quarters Load.

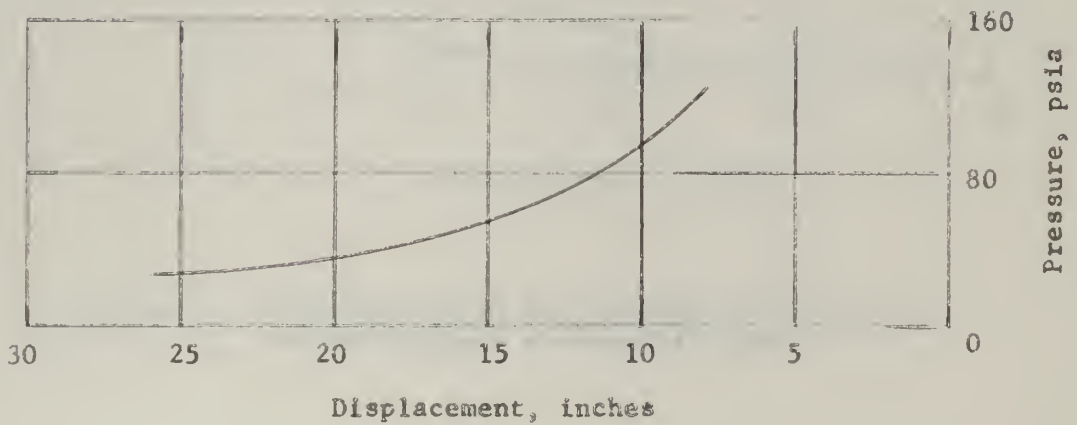


Figure 16. Pressure versus Displacement Diagram for Bounce Cylinder at Three-Quarters Load.

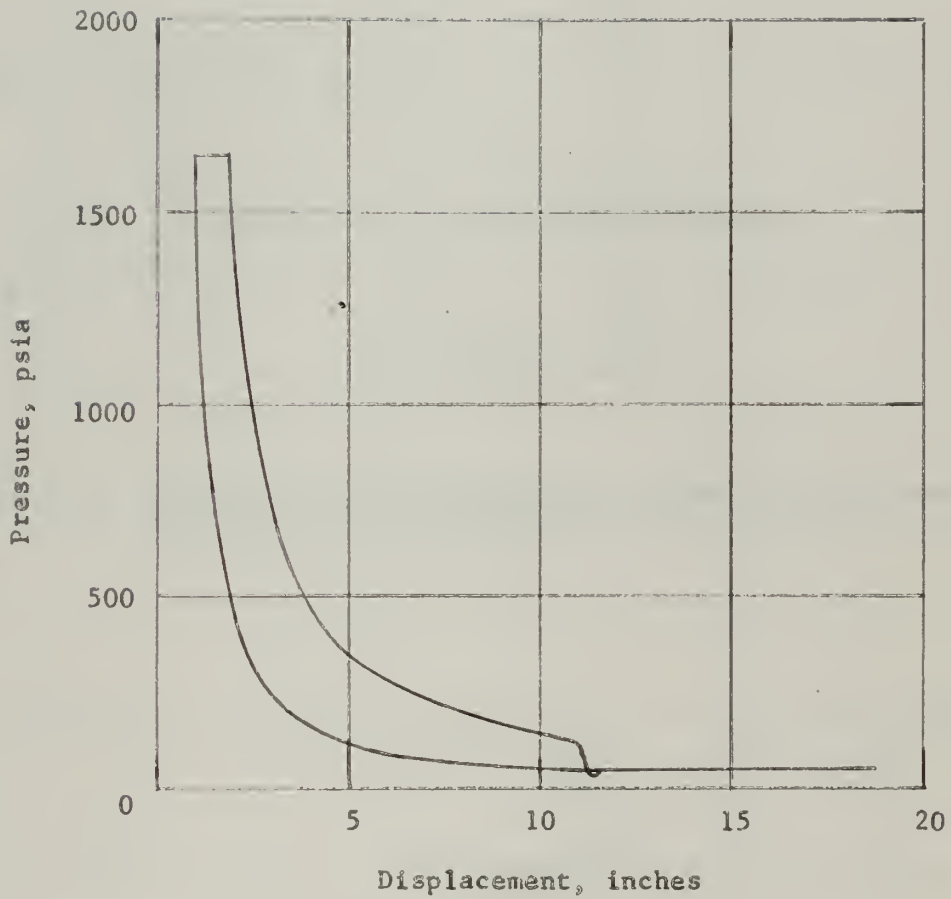


Figure 17. Pressure versus Displacement Diagram for Engine Cylinder at One-Half Load.

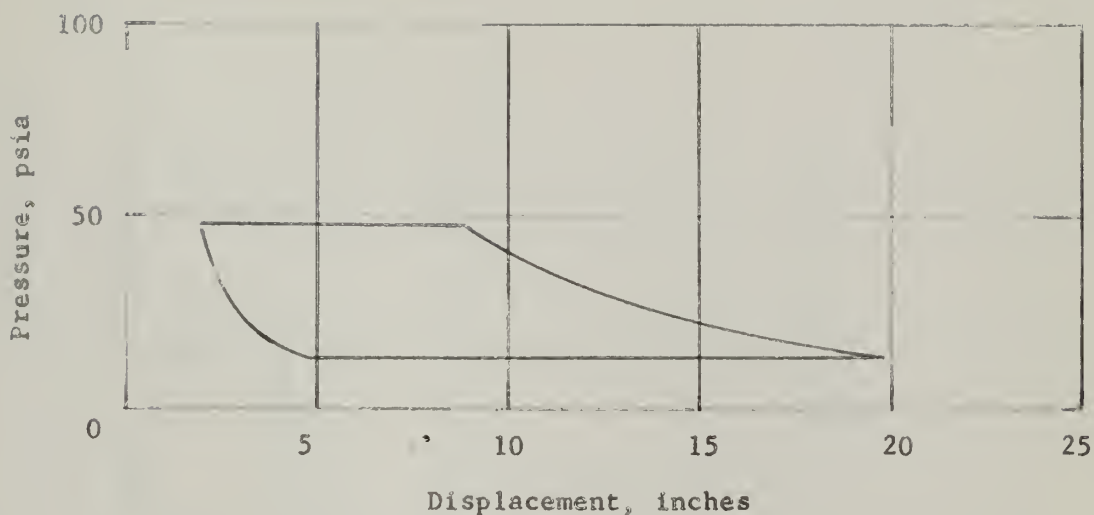


Figure 18. Pressure versus Displacement Diagram for Compressor Cylinder at One-Half Load.

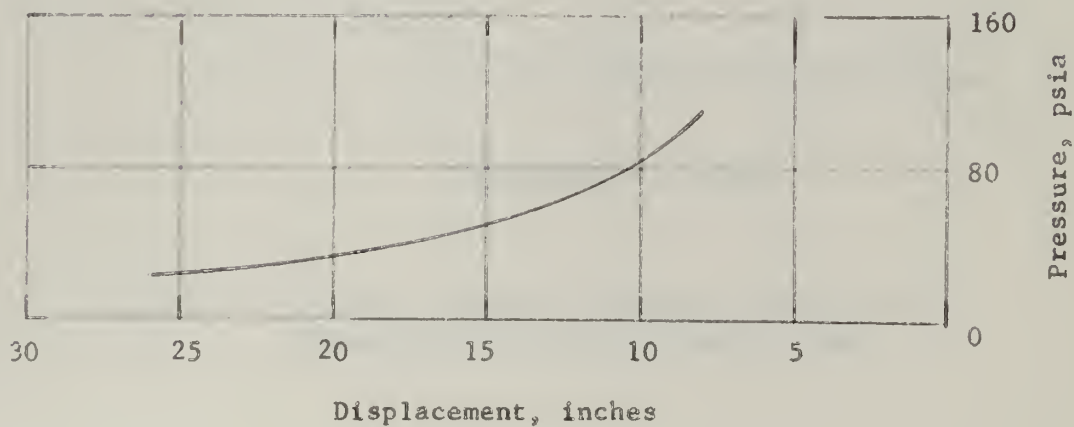


Figure 19. Pressure versus Displacement Diagram for Bounce Cylinder at One-Half Load.

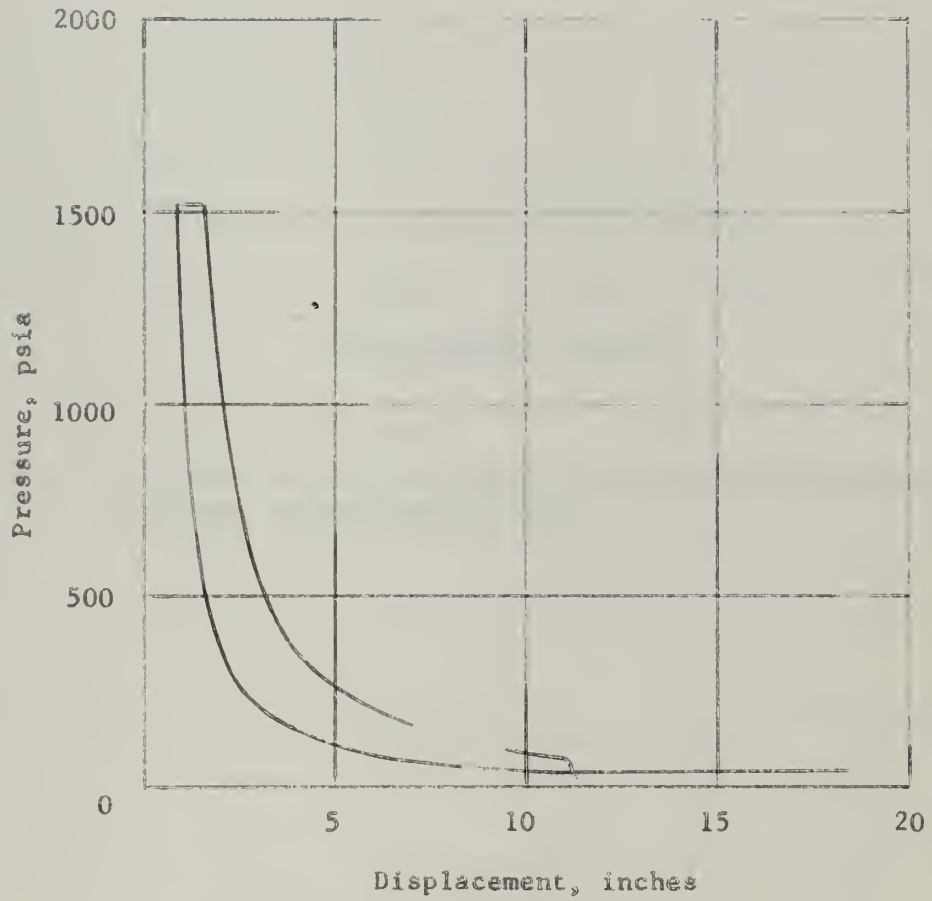


Figure 20. Pressure versus Displacement Diagram for Engine Cylinder at One-Quarter Load.

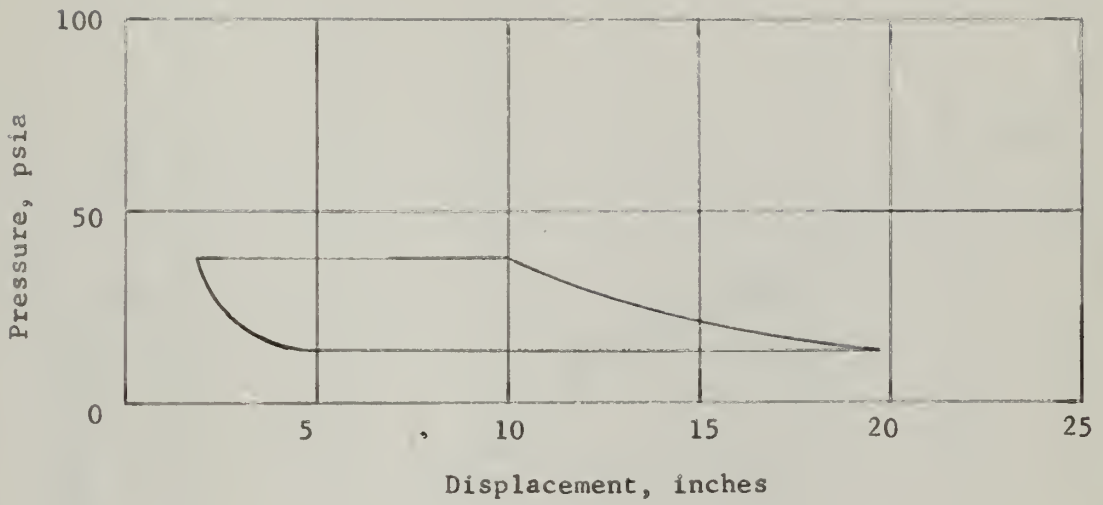


Figure 21. Pressure versus Displacement Diagram for Compressor Cylinder at One-Quarter Load.

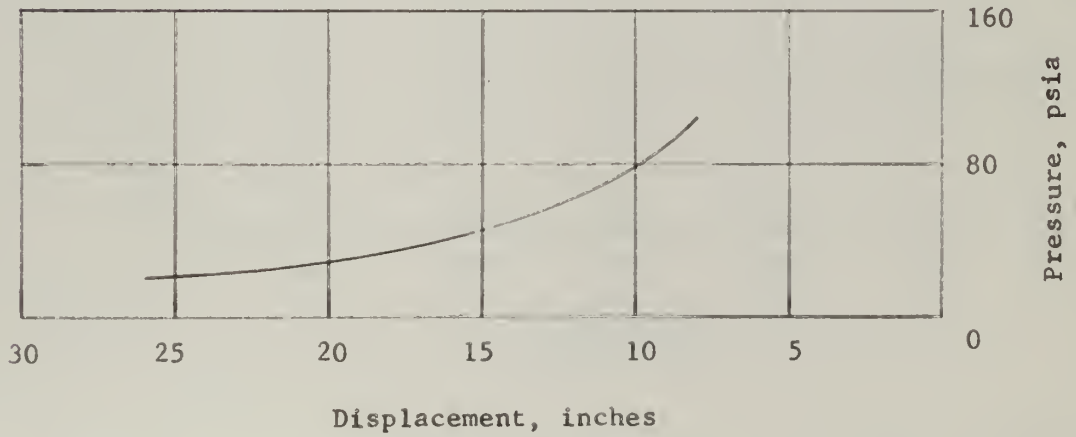


Figure 22. Pressure versus Displacement Diagram for Bounce Cylinder at One-Quarter Load.

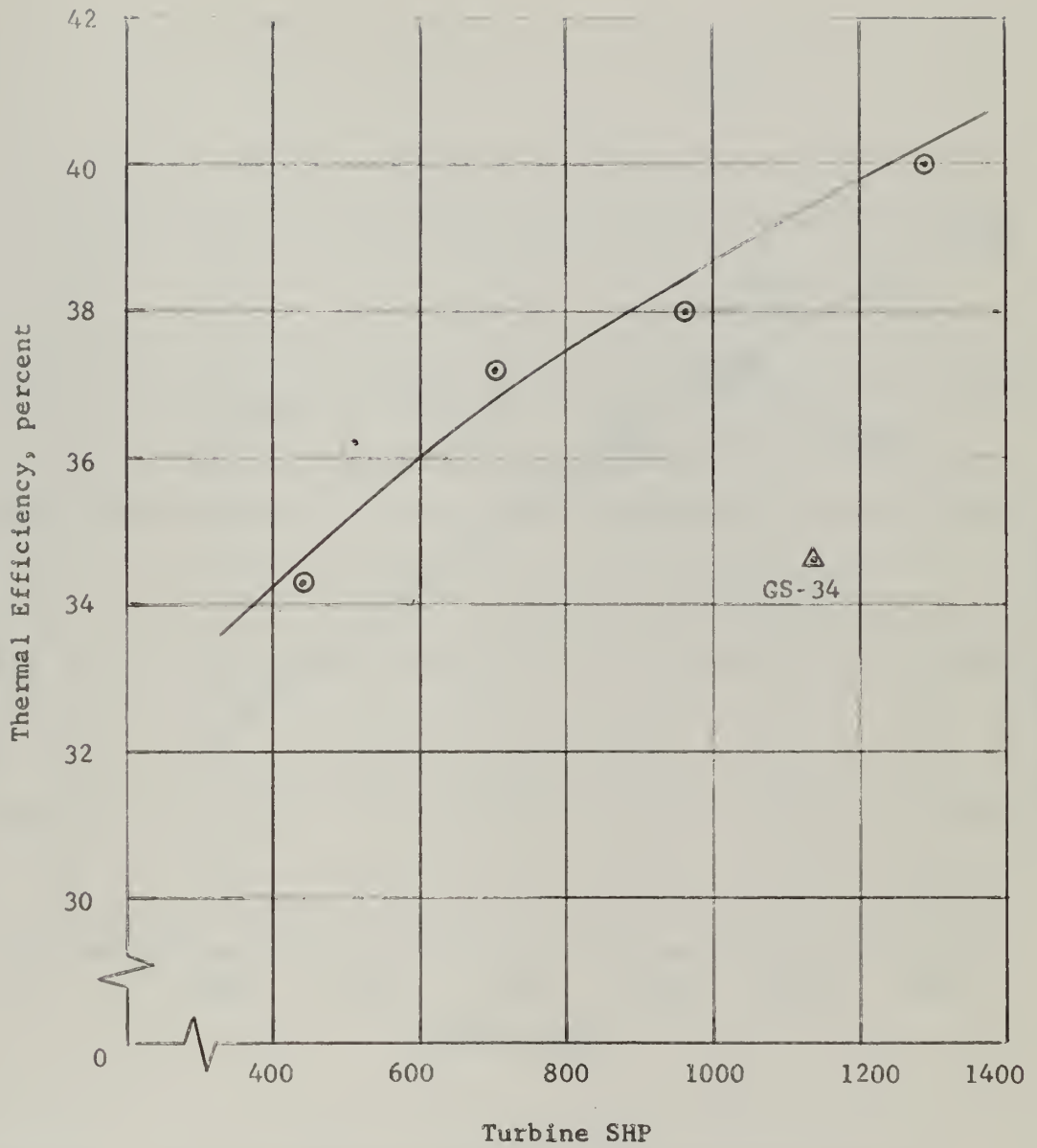


Figure 23. Thermal Efficiency on LHV Basis of Combined Gasifier-Turbine System versus Load from Computer Solution Results.

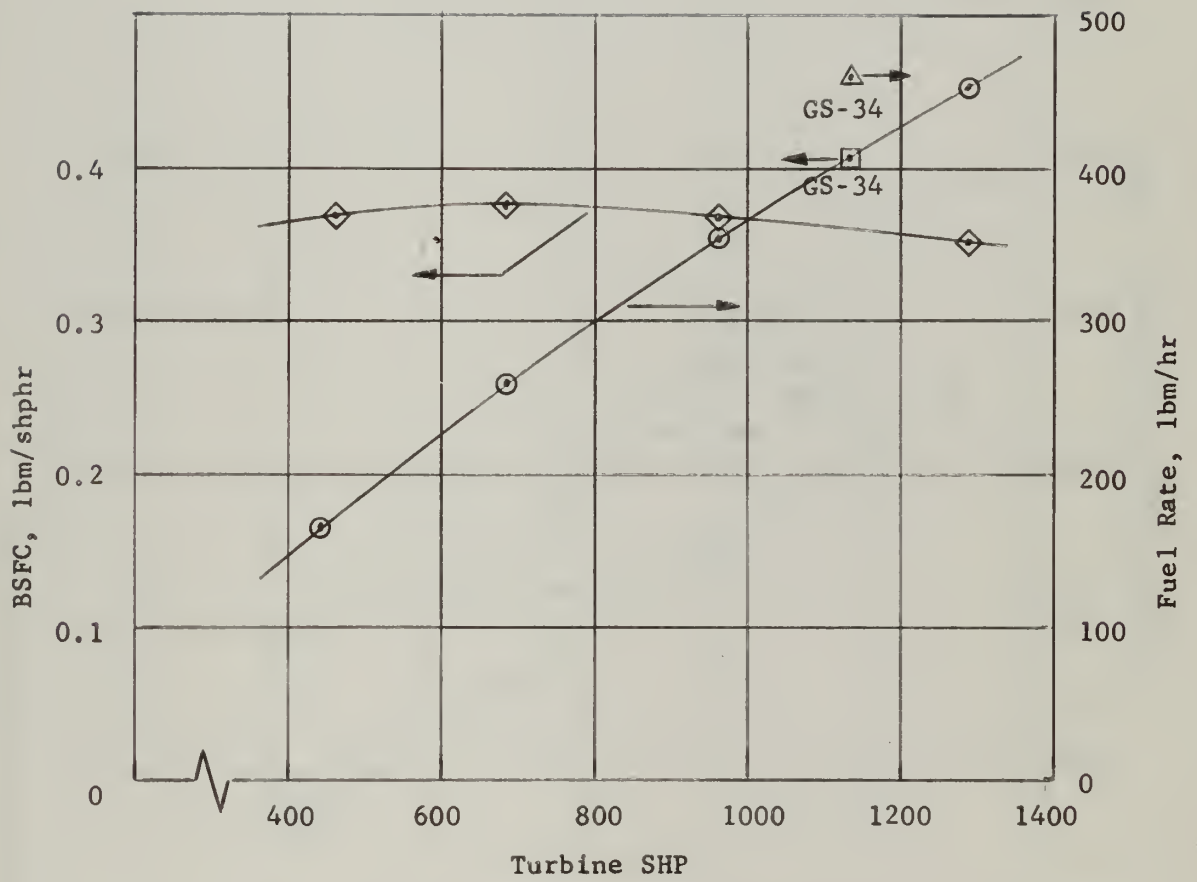


Figure 24. Fuel Consumption versus Load from Computer Solution Results.

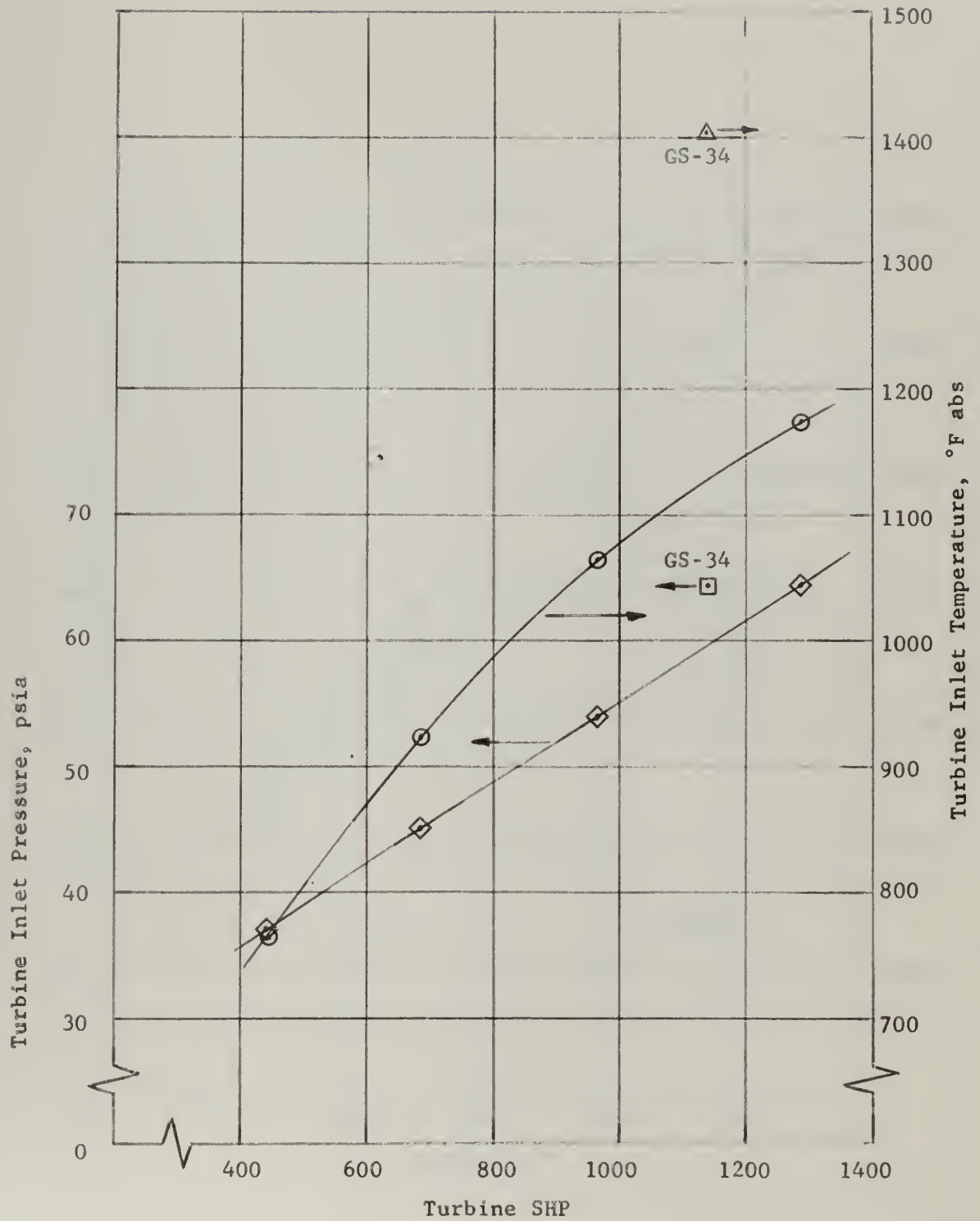


Figure 25. Turbine Inlet Pressure and Temperature versus Load from Computer Solution Results.

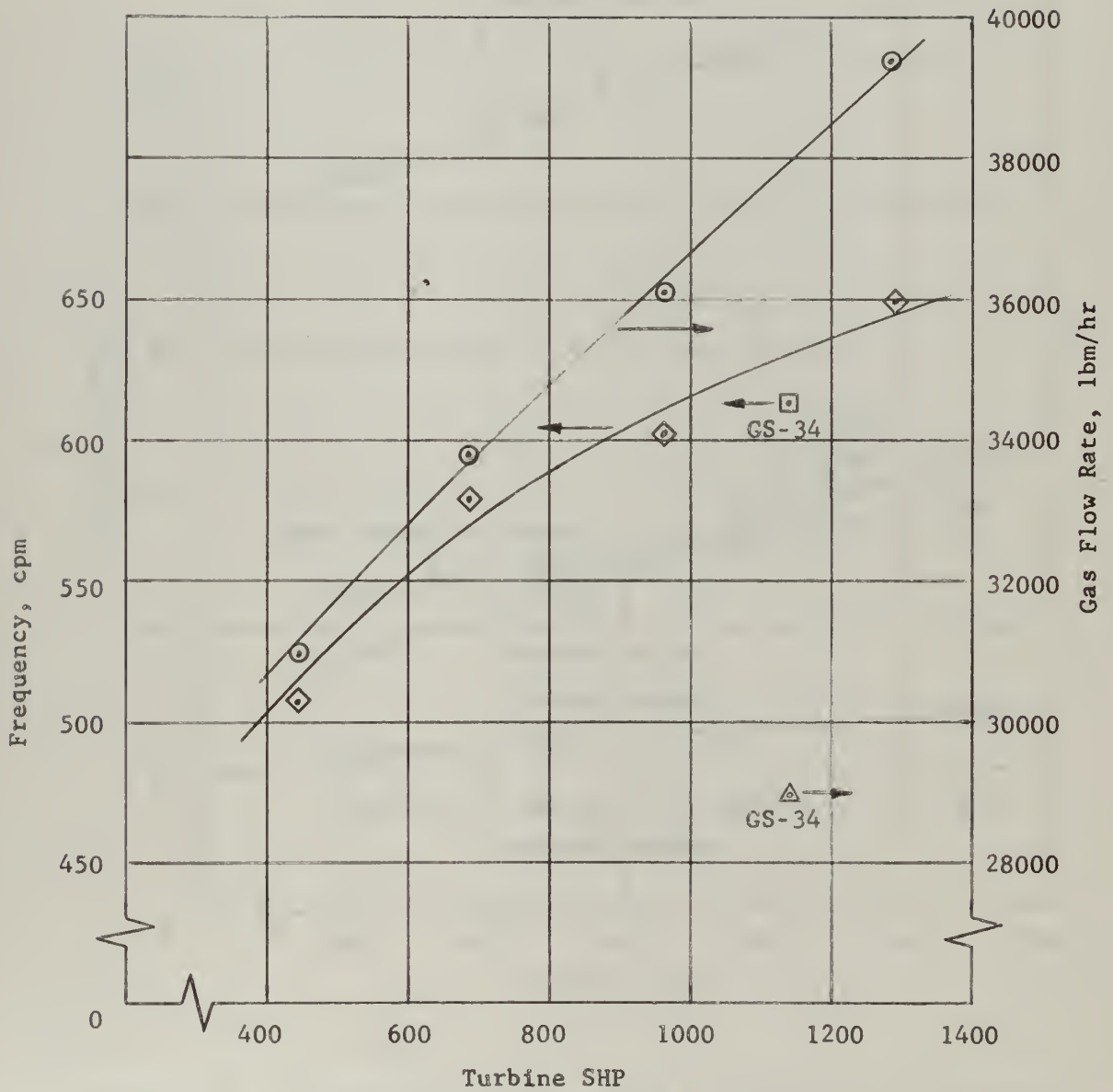


Figure 26. Frequency and Gas Flow Rate versus Load from Computer Solution Results.

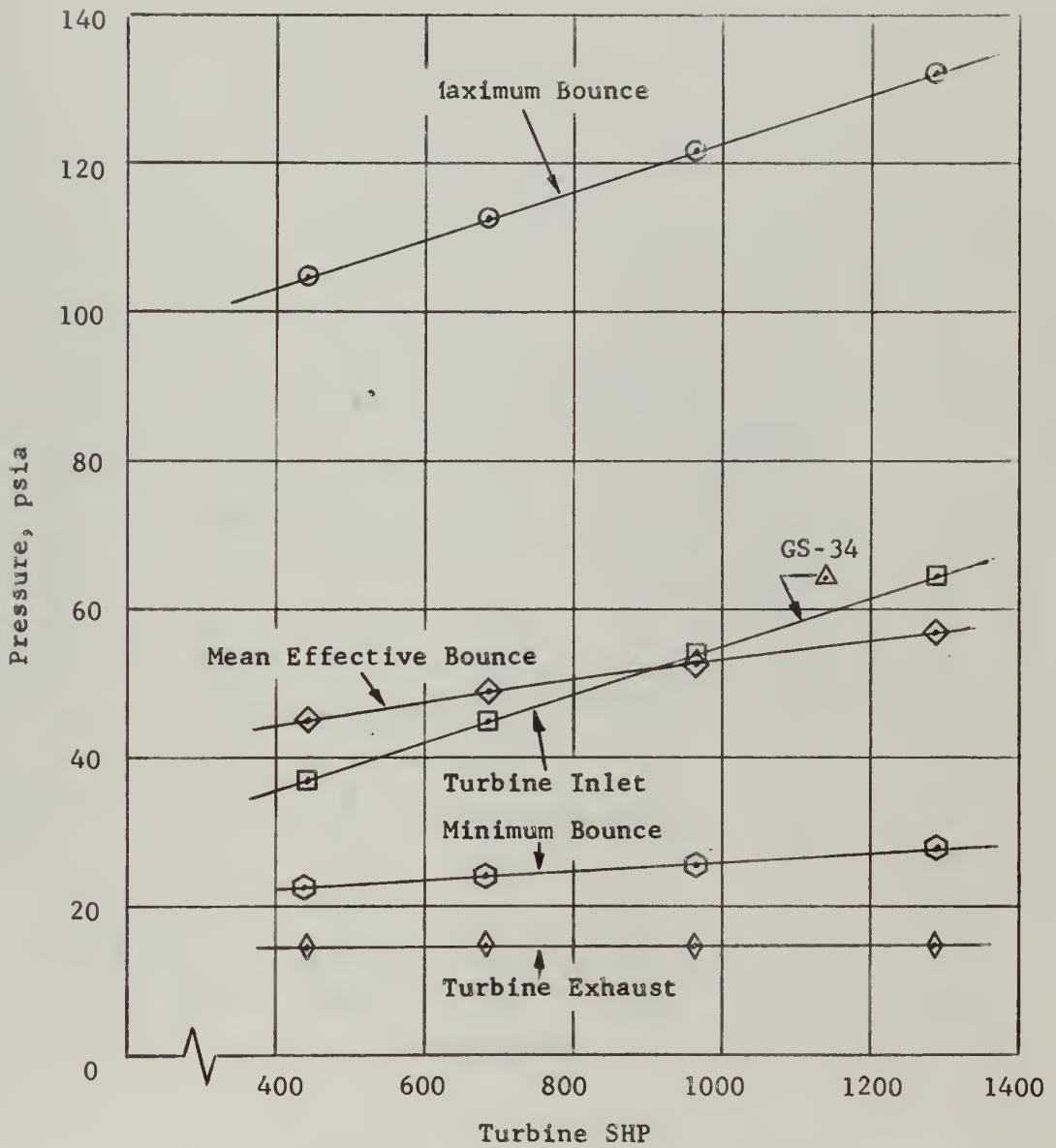


Figure 27. Operating Pressures versus Load Employed in Computer Simulation of SIGMA GS-34 Gas Generator.

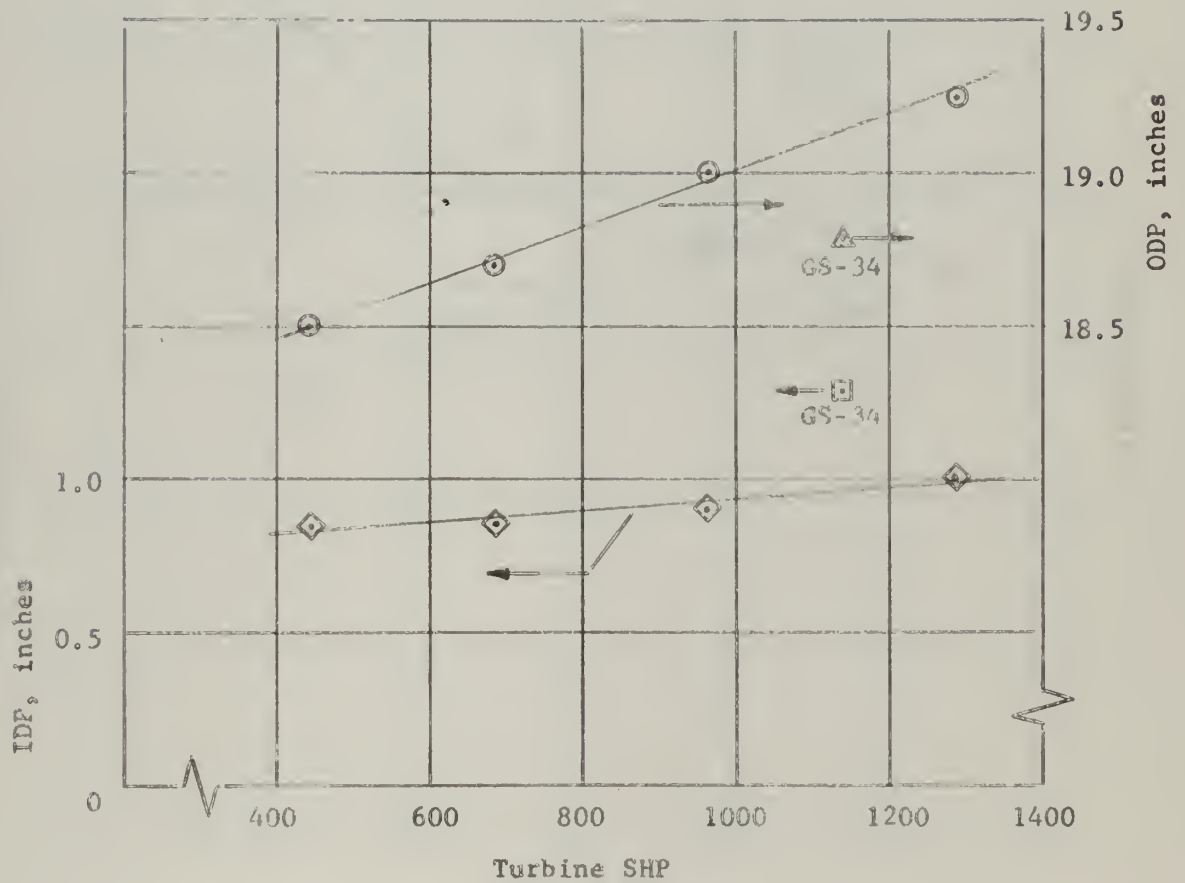


Figure 28. Inner and Outer Dead Points as Measured from Midpoint of Engine Cylinder versus Load from Computer Solution Results.

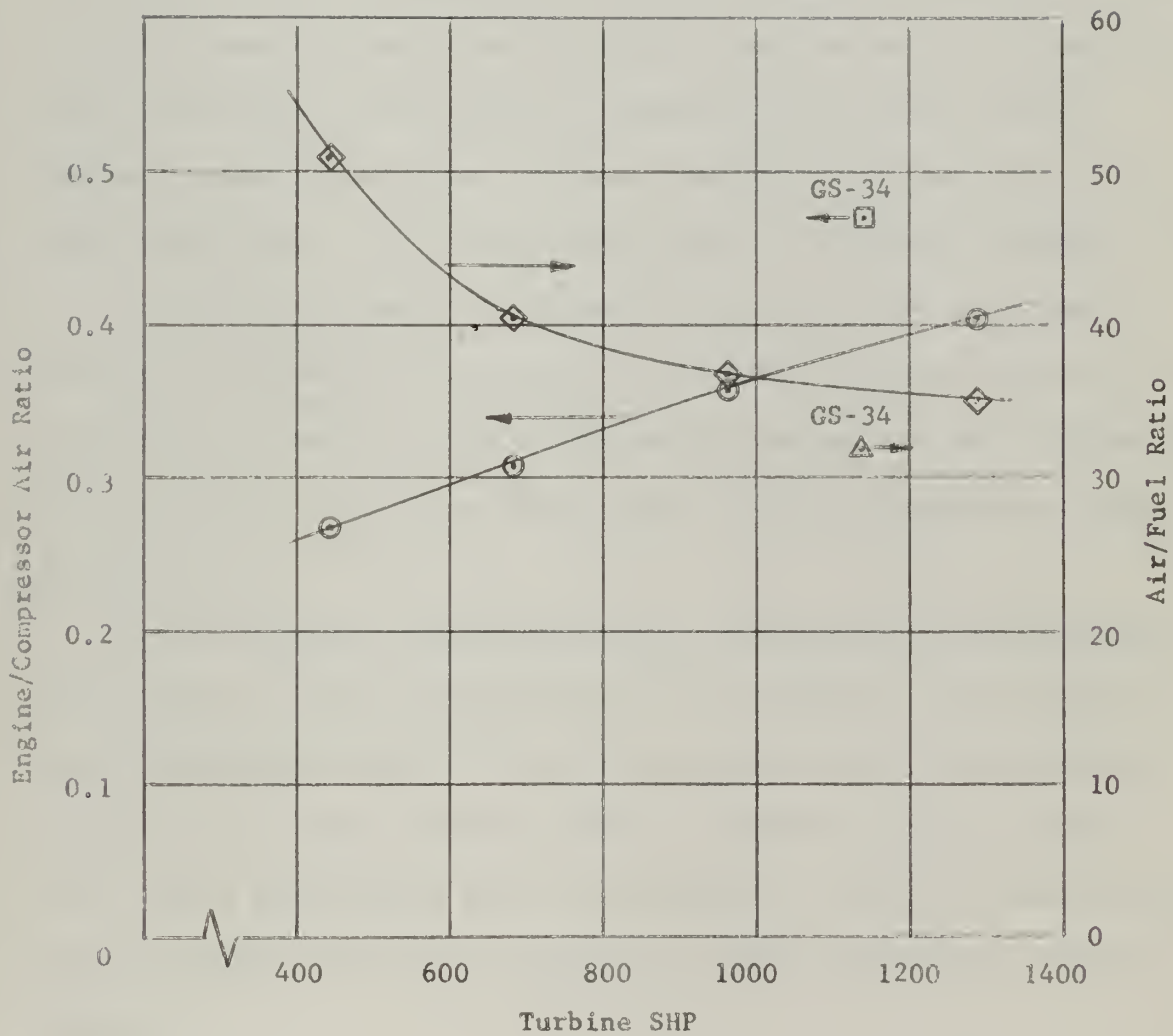


Figure 29. Ratio of Air/Fuel and Engine/Compressor Air versus Load from Computer Solution Results.

13. Conclusions.

The employment of single quadrant multiplication in the various computing loops resulted in uniform and stable operation of the analog circuit as a whole. However, the lack of automatic balancing permitted a certain amount of amplifier drift which could account for appreciable errors during the time required to complete a particular load run. Engine, compressor and bounce cylinder indicator diagrams had to be taken individually on the single available X - Y variable plotter.

In comparing computer solution results with actual performance data for the SIGMA GS-34 gasifier at full load condition (section 12), consideration should be made of the various assumptions and idealizations in constructing the analog circuit, particularly in the type of engine cycle employed.

Quite possibly a further refinement in this type of an investigation would be to adjust appropriate circuit parameters such as polytropic exponents to make the full load analog results come in closer agreement with actual performance data. With the resulting analog more closely simulating a given gas generator's operating characteristics, a more accurate analysis or prediction of part load behavior could be expected.

The performance data obtained from computer solution results for the various load conditions as tabulated in section 12 and graphically represented in Figs. 23 through 29 are considered reasonable for the operating conditions or criteria established for making the runs. The flexibility of the free piston system would permit a large variation of

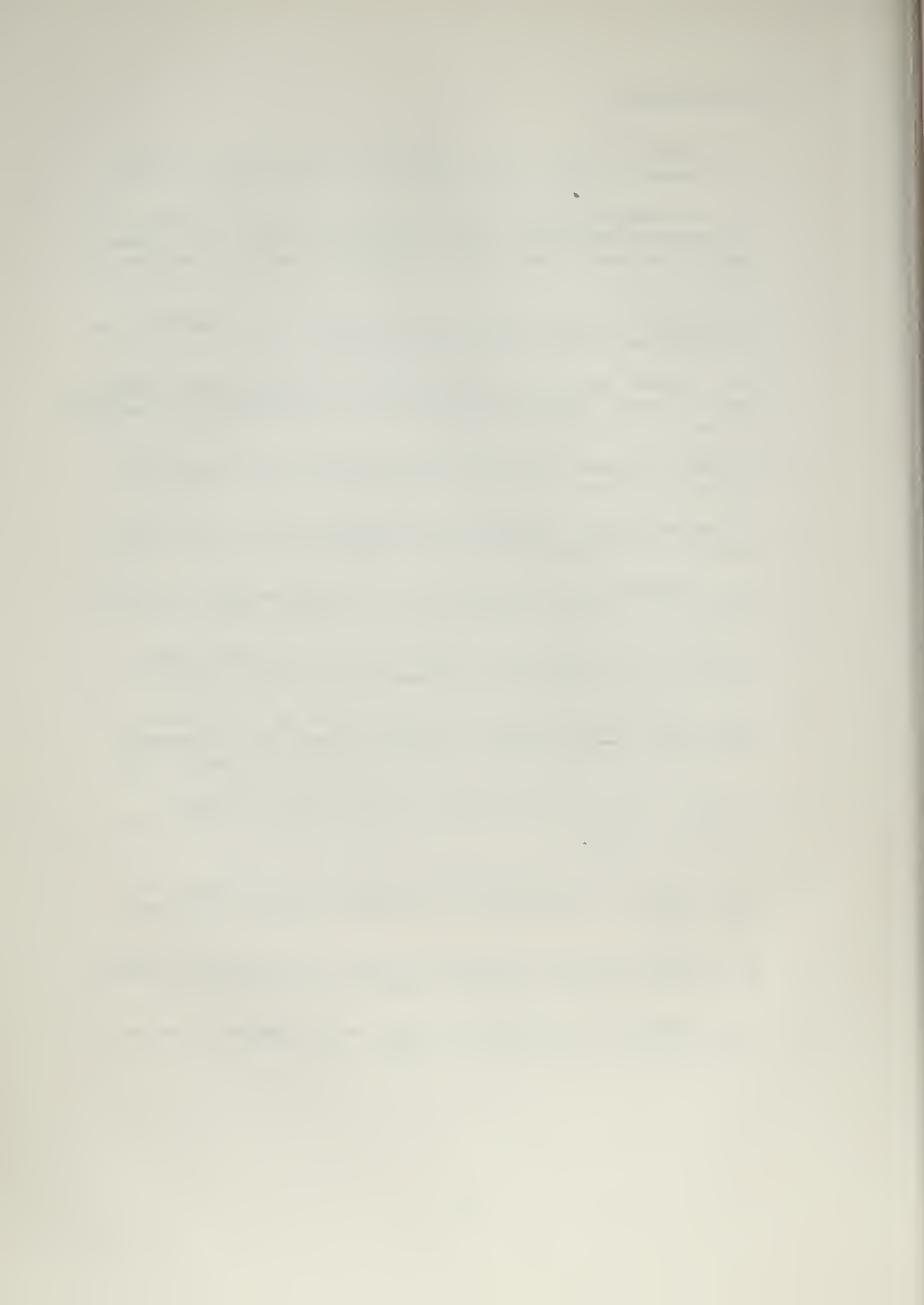
running conditions for a given output.

In the full and part load performance studies of the gas generator-turbine system of the previous section, no consideration was made of the flow characteristics of the turbine coupled to the gasifier. In actual practice to avoid losses by throttling between the gasifier and turbine it would be necessary to match the delivery of the gasifier with the consumption of the turbine. This is required since, with a given turbine, for each gas pressure there corresponds a particular mass flow. A particular mass flow requirement at a given delivery pressure from a gas generator would fix its stroke length.

This investigation has demonstrated that the operation of a free piston gas generator may be simulated to a reasonable degree of accuracy and stability by electronic analog means. By more closely approximating the various cycles of the actual machine, it is considered that the analog method could be an important means of predicting the performance of free-piston engine systems.

14. Bibliography

1. A. E. PLOW, LT, U. S. NAVY, Electronic Analog of a Free Piston Gas Generator, Thesis, U. S. Naval Postgraduate School, 1959.
2. A. K. OPPENHEIM and A. L. LONDON, The Free-Piston Gas Generator - A Thermodynamic-Dynamic Analysis, Technical Report FP-1, Department of Mechanical Engineering, Stanford University, February 15, 1950.
3. G. EICHELBERT, Free-Piston Generators, Part III - Appendix 1. of OPPENHEIM and LONDON Technical Report FP-1.
4. A. L. LONDON and A. K. OPPENHEIM, The Free-Piston Engine Development - Present Status and Design Aspects, Transactions of the ASME, Volume 74, pp. 1349-1361, 1952.
5. R. HUBER, Present State and Future Outlook of the Free-Piston Engine, ASME Paper No. 58-GTP-9, 1958.
6. M. BARTHALON and H. HORGEN, French Experience with Free-Piston Gasifiers, ASME Paper No. 56-A-209, 1956.
7. A. R. BOBROWSKY, Analytical Methods for Performance Estimates of Free-Piston Gasifiers, ASME Paper No. 57-GTP-6, 1957.
8. G. FLYNN, Observations on 25,000 Hours of Free-Piston-Engine Operation, SAE Transactions, Volume 65, pp. 508-515, 1957.
9. A. L. LONDON, Part-Load Characteristics for the Free-Piston-and-Turbine Compound Engine, Technical Report FP-5, Department of Mechanical Engineering, Stanford University, November, 1957.
10. R. HUBER, Operational Stability of Free Piston Gasifiers, Journal of the American Society of Naval Engineers, Volume 62, pp. 259-272, 1950.
11. A. L. LONDON, The Free-Piston-and-Turbine Compound Engine-A Cycle Analysis, Transactions of the ASME, Volume 77, pp. 197-210, 1955.
12. L. C. LICHTY, Internal Combustion Engines, Sixth Edition, McGraw-Hill Book Co., New York, N. Y., 1951.
13. G. A. KORN and T. M. KORN, Electronic Analog Computers, McGraw-Hill Book Co., New York, N. Y., 1956.



14. Instruction Manual Model DL Baldwin-Lima-Hamilton Free Piston Gasifier-Turbine Propulsion Power Plant, U. S. Navy Contract: NObs-2699, Baldwin-Lima-Hamilton Corporation, Hamilton, Ohio, October, 1956.
15. Boeing Electronic Analog Computer Maintenance Manual, Model 7000 B, Document No. D-15487, Boeing Airplane Company, Seattle, Washington, August 1954.

APPENDIX I

TIME AND MAGNITUDE SCALING

With the exception of the scaling for the friction analog, the same time and magnitude scaling relations as developed in Plow [1] apply to the computer circuitry of this investigation. These scaling relations with respect to the circuit components of Fig. 10 are given below:

1. Engine pressure, compressor pressure, bounce pressure and displacement integrating amplifiers (Nos. 1, 8, 12 and 19 respectively),

$$\frac{a_1}{R_1 C f_1} = \frac{a_8}{R_8 C f_8} = \frac{a_{12}}{R_{12} C f_{12}} = \frac{a_{19}}{R_{19} C f_{19}} = \frac{\alpha \ddot{x}}{\alpha \dot{x} \alpha t}$$

Within the computing loops simulating engine, compressor, and bounce pressures, magnitude scales involved in the multiplications and divisions are fixed as described in sections 6, 7 and 8. Scaling is required only for the above pressure integrating amplifiers.

2. Summation of forces amplifier (No. 17)

$$\frac{a_{171} R_{f17}}{R_{171}} = \frac{A_e \alpha P_e}{M \alpha \ddot{x}}$$

$$\frac{a_{172} R_{f17}}{R_{172}} = \frac{A_c \alpha P_c}{M \alpha \ddot{x}}$$

$$\frac{a_{173} R_{f17}}{R_{173}} = \frac{A_b \alpha P_b}{M \alpha \ddot{x}}$$

and

$$\frac{a_{174} R_{f17}}{R_{174}} = \frac{\alpha F_{fr}}{M \alpha \ddot{x}}$$

3. Velocity integrating amplifier (No. 18),

$$\frac{a_{18}}{R_{18} C f_{18}} = \frac{\alpha \dot{x}}{\alpha \dot{x} \alpha t}$$

The above scaling relations together with fixed circuit quantities as shown in Figs. 6, 7, 8 and 9 are all that are required for the complete analog network of Fig. 10.

APPENDIX II

PROGRAMMING ANALOG COMPUTER FOR SIGMA GS-34

FREE-PISTON GAS GENERATOR - FULL AND PART LOAD

Programming of the analog computer for the SIGMA GS-34 free-piston gas generator for full and part load conditions requires the following input parameters:

1. Fixed geometric parameters (references 2 and 4):

A_e	0.979 ft ²
A_c	5.73 ft ²
A_b	6.77 ft ²
M	1110 lbm
x_p	11.0 in
c	1.09 in
b	26.92 in

2. Fixed operating parameter (section 3 and reference 2):

C	960 lbf
---	---------

3. Variable operating parameters (references 2, 4 and 6 and section 13):

	Percent of Full Load			
	100	75	50	25
P_i , psia	14.0	14.0	14.0	14.0
P_d , psia	67.9	56.7	47.2	38.9
P_t , psia	64.5	54.0	45.0	37.0
P_b^0 , psia	132.3	121.8	112.8	104.8

4. Assumed polytropic exponents:

n_e	1.30
n'_e	1.40
n_b	1.40
n_c	1.30

The various scale factors required for the problem are assigned values as follows:

$$\begin{aligned} \alpha_{P_e} &= 50 \text{ psia/volt} = 7200 \text{ psfa/volt} \\ \alpha_{P_c} &= 5 \text{ psia/volt} = 720 \text{ psfa/volt} \\ \alpha_{P_b} &= 8 \text{ psia/volt} = 1152 \text{ psfa/volt} \\ \alpha_{F_{fr}} &= 80 \text{ lbf/volt} \\ \alpha_x &= 0.5 \text{ in/volt} = 1/24 \text{ ft/volt} \\ \alpha_{\dot{x}} &= 2 \text{ ft/sec/volt} \\ \alpha_{\dot{x}^2} &= 100 \text{ ft/sec}^2/\text{volt} \\ \alpha_t &= 100 \text{ sec computer time/1 sec real time} \end{aligned}$$

Based on the above scale factors, computer voltages corresponding to the geometric and operating input parameters and known as barred quantities are listed below:

\bar{x}_p	22.0				
\bar{c}	2.18				
\bar{b}	53.84				
\bar{C}	12.0				
		Percent of Full Load			
		100	75	50	25
\bar{P}_p	1.29	1.08	0.90	0.74	
\bar{P}_i	2.8	2.8	2.8	2.8	
\bar{P}_d	13.58	11.33	9.45	7.77	
\bar{P}_b^c	16.55	15.25	14.1	13.1	

Circuit components are determined from the scaling relationships of Appendix II as follows:

1. For pressure and displacement integrating amplifiers (Nos. 1, 8, 12 and 19),

$$\frac{a_1}{R_1 C_{f1}} = \frac{a_8}{R_8 C_{f8}} = \frac{a_{12}}{R_{12} C_{f12}} = \frac{a_{19}}{R_{19} C_{f19}} = \frac{\alpha \dot{x}}{\alpha_x \alpha_t} = 0.480$$

$$R's = 1 \text{ meg}$$

$$C's = 1 \mu \text{fd}$$

$$a's = 0.480$$

2. For summation of forces amplifier (No. 17),

$$\frac{a_{171} R_{f17}}{R_{171}} = \frac{A_e \alpha p_e}{M \alpha \ddot{x}} = 2.044$$

$$\frac{a_{172} R_{f17}}{R_{172}} = \frac{A_c \alpha p_c}{M \alpha \ddot{x}} = 1.196$$

$$\frac{a_{173} R_{f17}}{R_{173}} = \frac{A_b \alpha p_b}{M \alpha \ddot{x}} = 2.262$$

$$\frac{a_{174} R_{f17}}{R_{174}} = \frac{\alpha F_{fr}}{M \alpha \ddot{x}} = 0.0232$$

$$R_{f17} = 1 \text{ meg}$$

$$R_{171} = 0.25 \text{ meg}; \quad a_{171} = 0.511$$

$$R_{172} = 0.5 \text{ meg}; \quad a_{172} = 0.598$$

$$R_{173} = 0.25 \text{ meg}; \quad a_{173} = 0.565$$

$$R_{174} = 10 \text{ meg}; \quad a_{174} = 0.232$$

3. For velocity integrating amplifier (No. 18)

$$\frac{a_{18}}{R_{18} C_{f18}} = \frac{\alpha \ddot{x}}{\alpha \dot{x} \alpha t} = 0.500$$

$$R_{18} = 1 \text{ meg}$$

$$C_{f18} = 1 \mu \text{fd}$$

$$a_{15} = 0.500$$

APPENDIX III

FULL AND PART LOAD PERFORMANCE CALCULATIONS

FROM COMPUTER SOLUTION RESULTS

Data from the computer solution results as obtained from the recording equipment for the various load runs is as follows:

1. For full load

From time recorder trace

Cycle period, computer time = 9.25 sec/cycle

From engine cylinder diagram, Fig. 11

$$\bar{x}_1 = 38.5 \text{ volts}$$

$$\bar{x}_3 = 2.0 \text{ volts, } \bar{P}_2 = 32.0 \text{ volts}$$

$$\bar{x}_4 = 4.5 \text{ volts}$$

$$\bar{P}_5 = 3.7 \text{ volts}$$

$$\text{Area} = 144.0 \text{ volts}^2$$

From compressor cylinder diagram, Fig. 12

$$\bar{y}_1 = 41.0 \text{ volts}$$

$$\bar{y}_3 = 4.0 \text{ volts}$$

$$\bar{y}_4 = 11.2 \text{ volts}$$

$$\text{Area} = 198.4 \text{ volts}^2$$

From bounce cylinder diagram, Fig. 13

$$\bar{z}_1 = 15.4 \text{ volts, } \bar{P}_1 = 132.3 \text{ volts}$$

$$\bar{z}_2 = 52.0 \text{ volts, } \bar{P}_2 = 3.5 \text{ volts}$$

$$\bar{P}_{\text{ave}} = 7.13 \text{ volts}$$

2. For three-quarters load

From time recorder trace

Cycle period, computer time = 9.9 sec/cycle

From engine cylinder diagram, Fig. 14

$$\bar{x}_1 = 38.0 \text{ volts}$$

$$\bar{x}_3 = 1.8 \text{ volts, } \bar{P}_2 = 32.0 \text{ volts}$$

$$\bar{x}_4 = 3.9 \text{ volts}$$

$$\bar{P}_5 = 3.0 \text{ volts}$$

$$\text{Area} = 121.6 \text{ volts}^2$$

From compressor cylinder diagram, Fig. 15

$$\bar{y}_1 = 40.2 \text{ volts}$$

$$\bar{y}_3 = 4.0 \text{ volts}$$

$$\bar{y}_4 = 11.0 \text{ volts}$$

$$\text{Area} = 171.2 \text{ volts}^2$$

From bounce cylinder diagram, Fig. 16

$$\bar{z}_1 = 15.8 \text{ volts, } \bar{P}_1 = 15.25 \text{ volts}$$

$$\bar{z}_2 = 52.0 \text{ volts, } \bar{P}_2 = 3.2 \text{ volts}$$

$$\bar{P}_{\text{ave}} = 6.64 \text{ volts}$$

3. For one-half load

From time recorder trace

Cycle period, computer time = 10.68 sec/cycle

From engine cylinder diagram, Fig. 17

$$\bar{x}_1 = 37.4 \text{ volts}$$

$$\bar{x}_3 = 1.7 \text{ volts, } \bar{P}_2 = 33.0 \text{ volts}$$

$$\bar{x}_4 = 3.3 \text{ volts}$$

$$\bar{P}_5 = 2.2 \text{ volts}$$

$$\text{Area} = 105.6 \text{ volts}^2$$

From compressor cylinder diagram, Fig. 18

$$\bar{y}_1 = 39.6 \text{ volts}$$

$$\bar{y}_3 = 3.9 \text{ volts}$$

$$\bar{y}_4 = 10.0 \text{ volts}$$

$$\text{Area} = 155.2 \text{ volts}^2$$

From bounce cylinder diagram, Fig. 19

$$\bar{z}_1 = 16.0 \text{ volts}, \quad \bar{P}_1 = 14.1 \text{ volts}$$

$$\bar{z}_2 = 52.0 \text{ volts}, \quad \bar{P}_2 = 3.0 \text{ volts}$$

$$\bar{P}_{\text{ave}} = 6.13 \text{ volts}$$

4. For one-quarter load

From time recorder trace

$$\text{Cycle period, computer time} = 11.6 \text{ sec/cycle}$$

From engine cylinder diagram, Fig. 20

$$\bar{x}_1 = 37.0 \text{ volts}$$

$$\bar{x}_3 = 1.7 \text{ volts}, \quad \bar{P}_2 = 30.2 \text{ volts}$$

$$\bar{x}_4 = 2.9 \text{ volts}$$

$$\bar{P}_5 = 1.5 \text{ volts}$$

$$\text{Area} = 83.2 \text{ volts}^2$$

From compressor cylinder diagram, Fig. 21

$$\bar{y}_1 = 39.2 \text{ volts}$$

$$\bar{y}_3 = 3.9 \text{ volts}$$

$$\bar{y}_4 = 9.8 \text{ volts}$$

$$\text{Area} = 115.2 \text{ volts}^2$$

From bounce cylinder diagram, Fig. 22

$$\bar{z}_1 = 16.2 \text{ volts}, \quad \bar{P}_1 = 13.1 \text{ volts}$$

$$\bar{z}_2 = 52.0 \text{ volts}, \quad \bar{P}_2 = 2.8 \text{ volts}$$

$$\bar{P}_{\text{ave}} = 5.64 \text{ volts}$$

Calculation of performance results from full load data

follows:

1. Frequency

Cycle period based on computer time

$$= 9.25 \text{ sec/cycle}$$

Frequency based on computer time

$$= 6.49 \text{ cycles/min}$$

Frequency based on real time

$$= 6.49 \times 100 = 649 \text{ cycles/min.}$$

2. Stroke and clearances

$$\text{Stroke} = (\bar{x}_1 - \bar{x}_3) \alpha_x = (38.5 - 2.0) 0.5$$

$$= 18.25 \text{ inches}$$

$$\text{Engine effective stroke} = (\bar{x}_2 - \bar{x}_3) \alpha_x$$

$$= (22.0 - 2.0) 0.5$$

$$= 10.0 \text{ inches}$$

$$\text{Engine clearance} = \bar{x}_3 (\alpha_x) = 2.0 \times 0.5$$

$$= 1.0 \text{ inches}$$

$$\text{Compressor clearance} = \bar{y}_3 (\alpha_y) = 4.0 \times 0.5$$

$$= 2.0 \text{ inches}$$

$$\text{Bounce clearance} = \bar{z}_1 (\alpha_z) = 15.4 \times 0.5$$

$$= 7.7 \text{ inches}$$

3. Compressor discharge air

From equation 5.4.4:

$$m_d = \frac{P_i A_c Y_i}{R T_o}$$

$$P_i = 14.0 \text{ psia}$$

$$A_c = 5.73 \text{ ft}^2$$

$$Y_i = (\bar{y}_1 - \bar{y}_4) \alpha_y \\ = (41.0 - 11.2) 0.5 = 14.9 \text{ in.}$$

$$T_0 = 530^\circ \text{R}$$

$$m_d = \frac{(14.0)(144)(5.73)(14.9)}{(53.3)(530)(12)} \\ = 0.507 \text{ lbm}$$

4. Engine intake air

From equation 5.4.2:

$$m_e = \frac{P_p V_p}{R T_0 \left(\frac{P_d}{P_i} \right)^{\frac{n_c - 1}{n_c}}}$$

$$P_p = 64.5 \text{ psia}$$

$$V_p = \frac{(11.0)(0.979)}{12} = 0.897 \text{ ft}^2$$

$$P_d = 67.9 \text{ psia}$$

$$P_i = 14.0 \text{ psia}$$

$$n_c = 1.30$$

$$m_e = \frac{(64.5)(144)(0.897)}{(53.3)(530)(4.85)^{0.30/1.30}} \\ = 0.205 \text{ lbm}$$

5. Ratio of engine to compressor air

$$m_e / m_d = 0.205 / 0.507$$

$$= 0.404$$

6. Fuel input

$$Q_f = m_f \text{LHV} = \frac{k}{k-1} P_3 (V_4 - V_3)$$

$$P_3 = \bar{P}_3 (\alpha_{P_e}) = 32.0 \times 50 \\ = 1600 \text{ psia}$$

$$\Delta V = \frac{(\bar{x}_4 - \bar{x}_3)(\alpha_x)(Ae)}{12} = \frac{(4.5 - 2.0)(0.5)(0.979)}{12}$$

$$= 0.102 \text{ ft}^3$$

$$Q_f = m_f \text{ LHV} = \frac{1.40}{0.40} (1600)(144)(0.102)$$

$$= 82,200 \text{ ft-lbf}$$

Assuming LHV = 18,200 BTU/lbm

$$m_f = \frac{82,200}{(18,200)(778)}$$

$$= 0.0058 \text{ lbm/cycle-side}$$

7. Air - fuel ratio

$$A/F = m_e / m_f = 0.205 / 0.0058$$

$$= 35.3$$

8. Fuel flow rate

$$\text{Fuel rate} = 2(m_f) (\text{fr}) (60)$$

$$= 2(0.0058) (649) (60)$$

$$= 452 \text{ lbm/hr}$$

9. Gas flow rate

$$\text{Gas rate} = 2(m_d) (\text{fr}) (60)$$

$$= 2(0.507) (649) (60)$$

$$= 39,400 \text{ lbm/hr}$$

10. Engine exhaust gas temperature

From equation 5.5.1:

$$T_e = \frac{T_5}{k} \left[1 + (k-1) \frac{P_6}{P_5} \right]$$

$$T_5 = \frac{P_5 V_5}{m_e R} = \frac{(185)(144)(0.897)}{(0.205)(53.3)} = 2,185^\circ R$$

$$T_e = \frac{2,185}{1.40} \left[1 + (1.40 - 1) \frac{64.5}{185} \right]$$

$$= 1,778^\circ R$$

11. Generator gas delivery temperature

From equation 5.5.3:

$$T_t = \frac{m_e}{m_d} T_e + \left(1 - \frac{m_e}{m_d}\right) T_p$$

$$T_p = T_o \left(\frac{P_d}{P_i}\right)^{\frac{n_c - 1}{n_c}} = 530 (4.85)^{\frac{0.30}{1.30}}$$

$$= 763 \text{ } ^\circ R$$

$$T_t = 0.404 (1,778) + (1 - 0.404) 763$$

$$= 1,174 \text{ } ^\circ R$$

12. Power output of the system

From the gas tables - air at low pressure for one pound - isentropic available energy, Δh_s , on expansion from state in item 11 to atmospheric pressure is equal to 97.8 BTU/lbm.

From equation 5.5.5:

$$(\text{shp})_{\text{turbine}} = \frac{(\Delta h_s)(778)(2)(m_d)(f_r)(n_t)}{33,000}$$

$$= \frac{(97.8)(778)(2)(0.507)(649)(0.85)}{33,000}$$

$$= 1290 \text{ hp}$$

13. Net work balance per engine cycle

From equation 3.3:

$$Wk_{\text{net eng}} = Wk_{\text{net comp}} + Wk_{\text{fr}}$$

$$Wk_{\text{net eng}} = (144.0)(7,200)(0.979)\left(\frac{1}{24}\right)$$

$$= 42,200 \text{ ft-lbf}$$

$$Wk_{\text{net comp}} = (198.4)(720)(5.73)\left(\frac{1}{24}\right)$$

$$= 34,100 \text{ ft-lbf}$$

$$Wk_{\text{fr}} = (2)(960)(18.25/12)$$

$$= 2,920 \text{ ft-lbf}$$

Discrepancy: 7180 ft-lbf or 17.0 percent on basis of net engine work.

14. Brake specific fuel consumption

$$\begin{aligned} \text{BSFC} &= m_f / (\text{shp})_{\text{turbine}} \\ &= 452/1,290 \\ &= 0.351 \text{ lbm/shphr} \end{aligned}$$

15. Engine indicated thermal efficiency, LHV basis

$$\begin{aligned} (\eta_{\text{th}})_{\text{engine}} &= \frac{(Wk_{\text{net}})_{\text{engine}}}{Q_f} \times 100 \\ &= \frac{42,200}{82,200} \times 100 \\ &= 51.3 \text{ percent} \end{aligned}$$

16. Overall thermal efficiency, LHV basis

$$\begin{aligned} (\eta_{\text{th}})_{\text{overall}} &= \frac{(\text{shp})(33,000)(100)}{(\dot{m}_f/60)(\text{LHV})(778)} \\ &= \frac{(1,290)(33,000)(100)}{(452/60)(18,200)(778)} \\ &= 39.8 \text{ percent} \end{aligned}$$

Above sample calculations represent the full load condition of the gas generator-turbine system. Performance results for part-load runs are tabulated in section 12 of the investigation.

APPENDIX IV

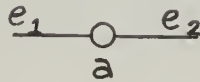
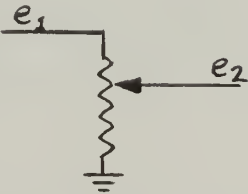
ANALOG COMPUTER SYMBOLS

Circuit

Symbol

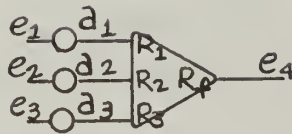
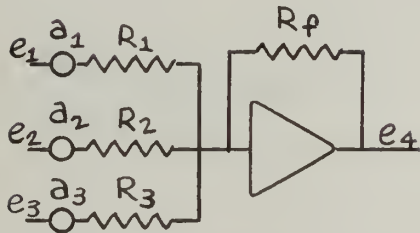
Function

1. Potentiometer:



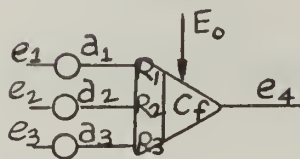
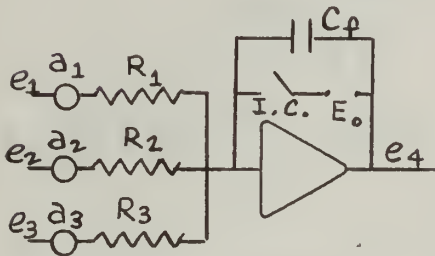
$$e_2 = a e_1$$

2. Summer:



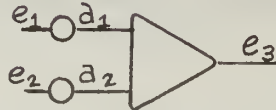
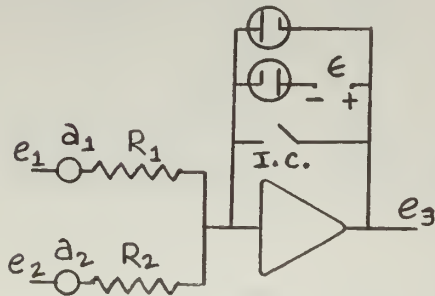
$$e_4 = - \left(\frac{a_1 R_f}{R_1} e_1 + \frac{a_2 R_f}{R_2} e_2 + \frac{a_3 R_f}{R_3} e_3 \right)$$

3. Summing Integrator:



$$e_4 = - \int_0^t \left(\frac{a_1}{R_1 C_f} e_1 + \frac{a_2}{R_2 C_f} e_2 + \frac{a_3}{R_3 C_f} e_3 \right) dt + E_0$$

4. Relay Driver:



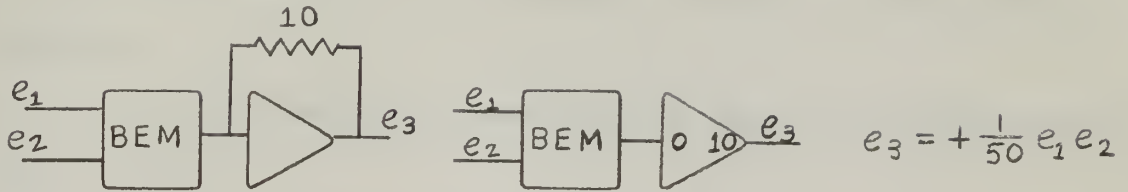
$$e_3 = \begin{cases} 0 & \text{when } \frac{a_1 e_1}{R_1} + \frac{a_2 e_2}{R_2} > 0 \\ +E & \text{when } \frac{a_1 e_1}{R_1} + \frac{a_2 e_2}{R_2} < 0 \end{cases}$$

Circuit

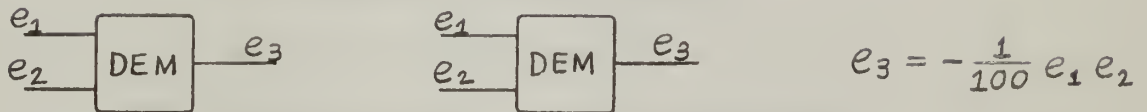
Symbol

Function

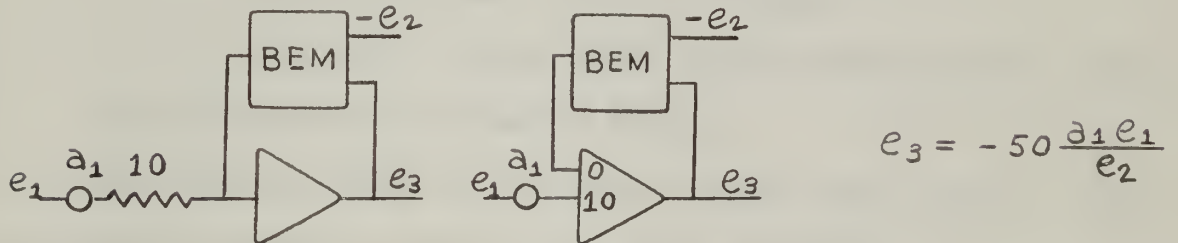
5. Boeing Electronic Multiplier:



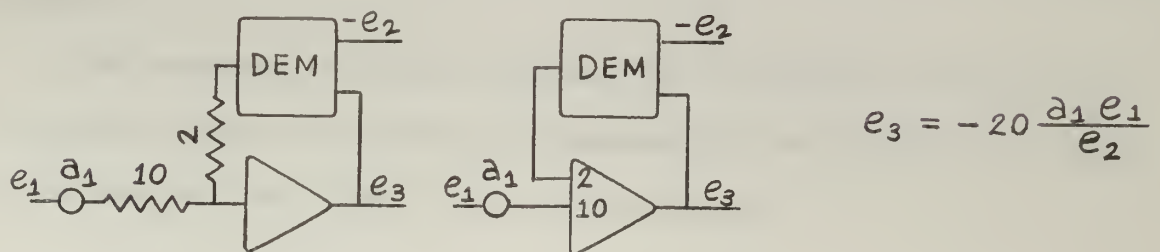
6. Donner Electronic Multiplier:



7. Division using Boeing Multiplier:



8. Division using Donner Multiplier:



In division circuits using Boeing and Donner multipliers, variable divisor voltage, e_2 , must always be negative for stable operation.

APPENDIX V

DESCRIPTION OF EQUIPMENT

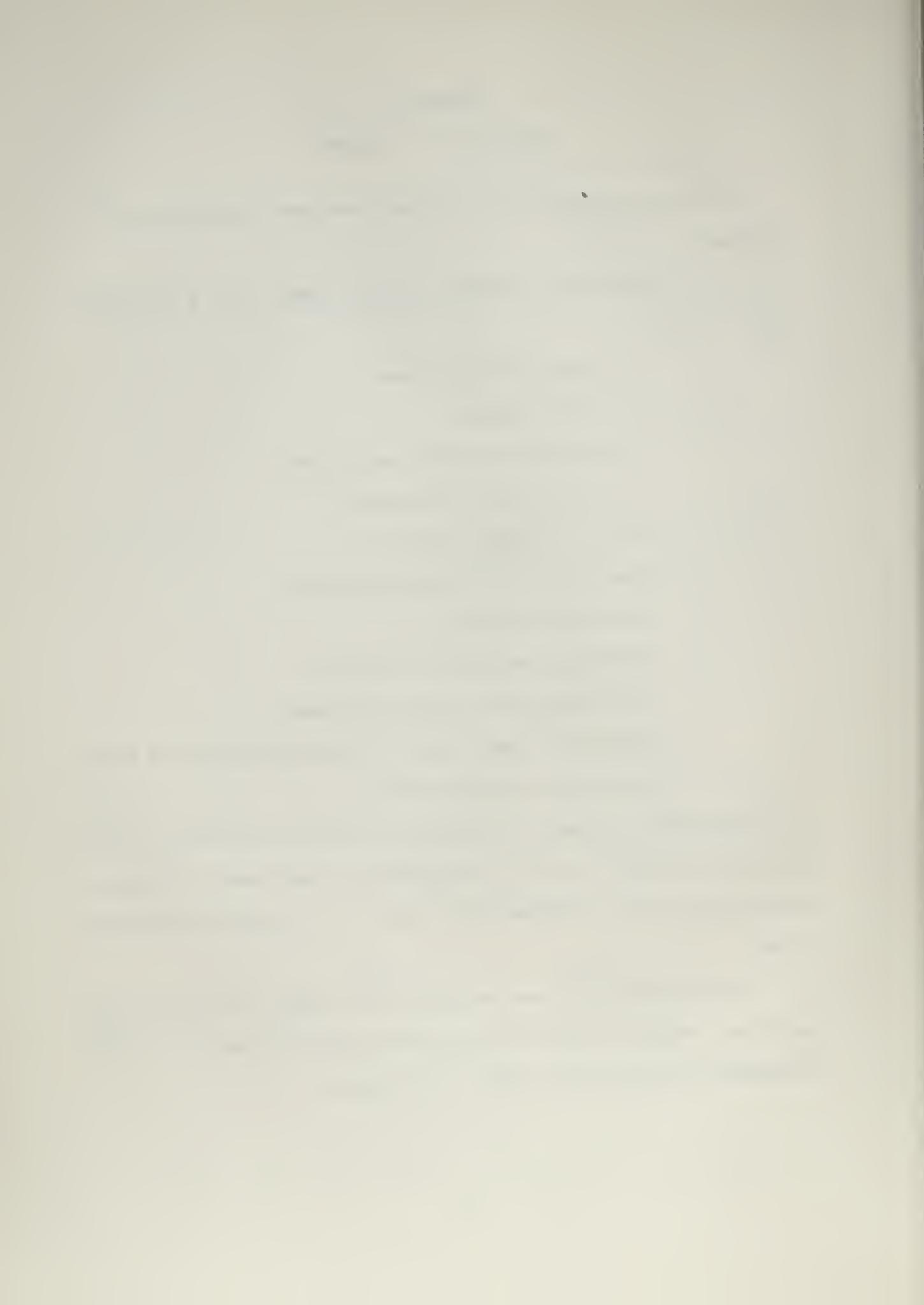
For this investigation the following equipment components were employed:

1. Two Boeing electronic computer (BEAC) racks [15] containing:
 - a. Operational amplifiers.
 - b. Diode limiters.
 - c. Electronic function multipliers.
 - d. Coefficient potentiometers.
 - e. I. C. voltage source.
2. Donner electronic function multipliers.
3. Sanborn time recorder.
4. Electronics Associates X-Y plotter.
5. Electro Instruments digital voltmeter.
6. Single pole, double throw, non-polarized sensitive relays.

The above equipment is shown in Fig. 31.

The computing network for simulation of the free-piston gas generator problem required a total of 25 operational amplifiers, 6 electronic function multipliers, 11 diode tube limiters and 10 sensitive switching relays.

The switching relays were actuated by the output of an operational amplifier. Amplifier feed-back arrangement and connection of the relay energizing coil are shown in Fig. 20 next page.



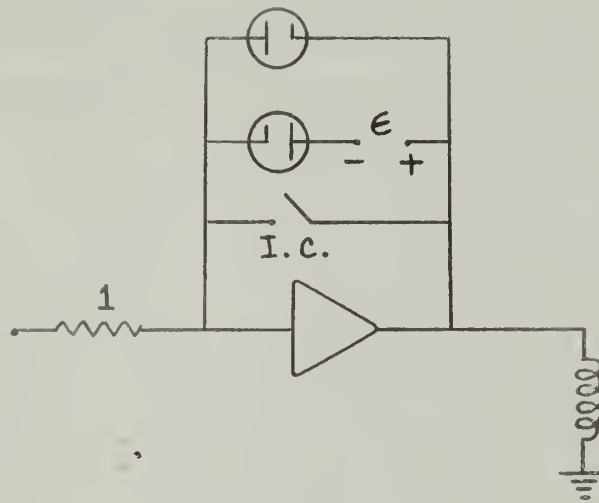


Figure 30. Actuation of Relays.

Sensitive relays available for this investigation were of the single pole, double throw, non-polarized type. With no energizing voltage, one of the two sets of contact points would be closed by spring action. When actuated, contact between the other set of points would be made against the spring force.

As indicated in Fig. 30 the feedback of the relay driver amplifier consisted of diode limiters and a bias voltage, ϵ . A positive voltage signal at the grid of the amplifier would effectively clamp the output of the amplifier to ground potential resulting in an unactuated condition of the relay. A negative input of any magnitude on the other hand would result in an amplifier output determined by the bias voltage thereby actuating the relay. Bias voltage was adjusted to a value sufficient to operate the relays but not to exceed the maximum 10 milliamperes ratings of the amplifiers.

The above principle was employed for the actuation of all relays identified by the subscript "R" in the computing circuit of Fig. 10. In this figure the eight \dot{x} relays (energizing coils all in series) were actuated by Amplifier 21, x_p relay by Amplifier 23 and Q_f relay by Amplifier 7.

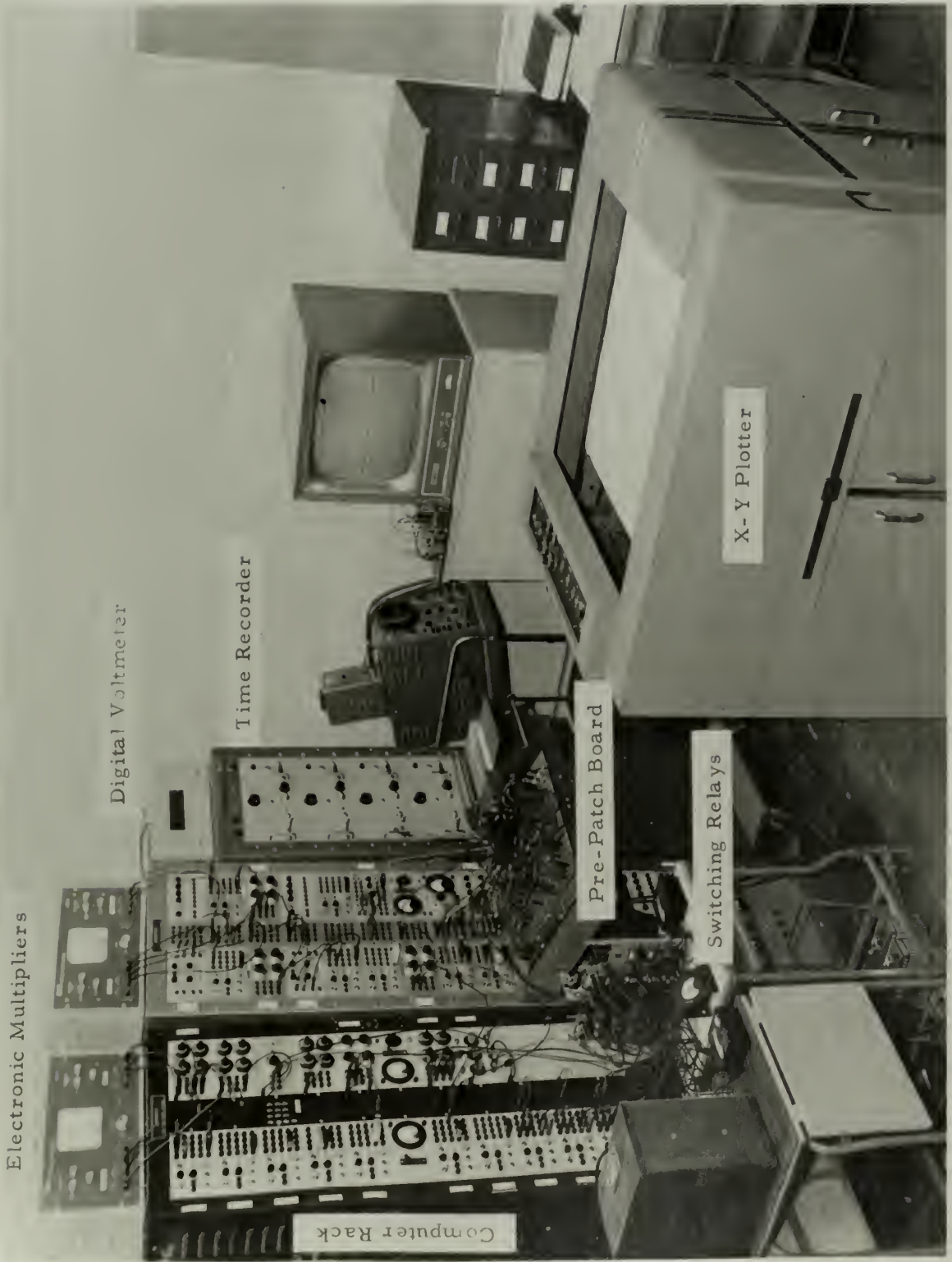


Figure 31. Equipment Components Employed in Investigation.